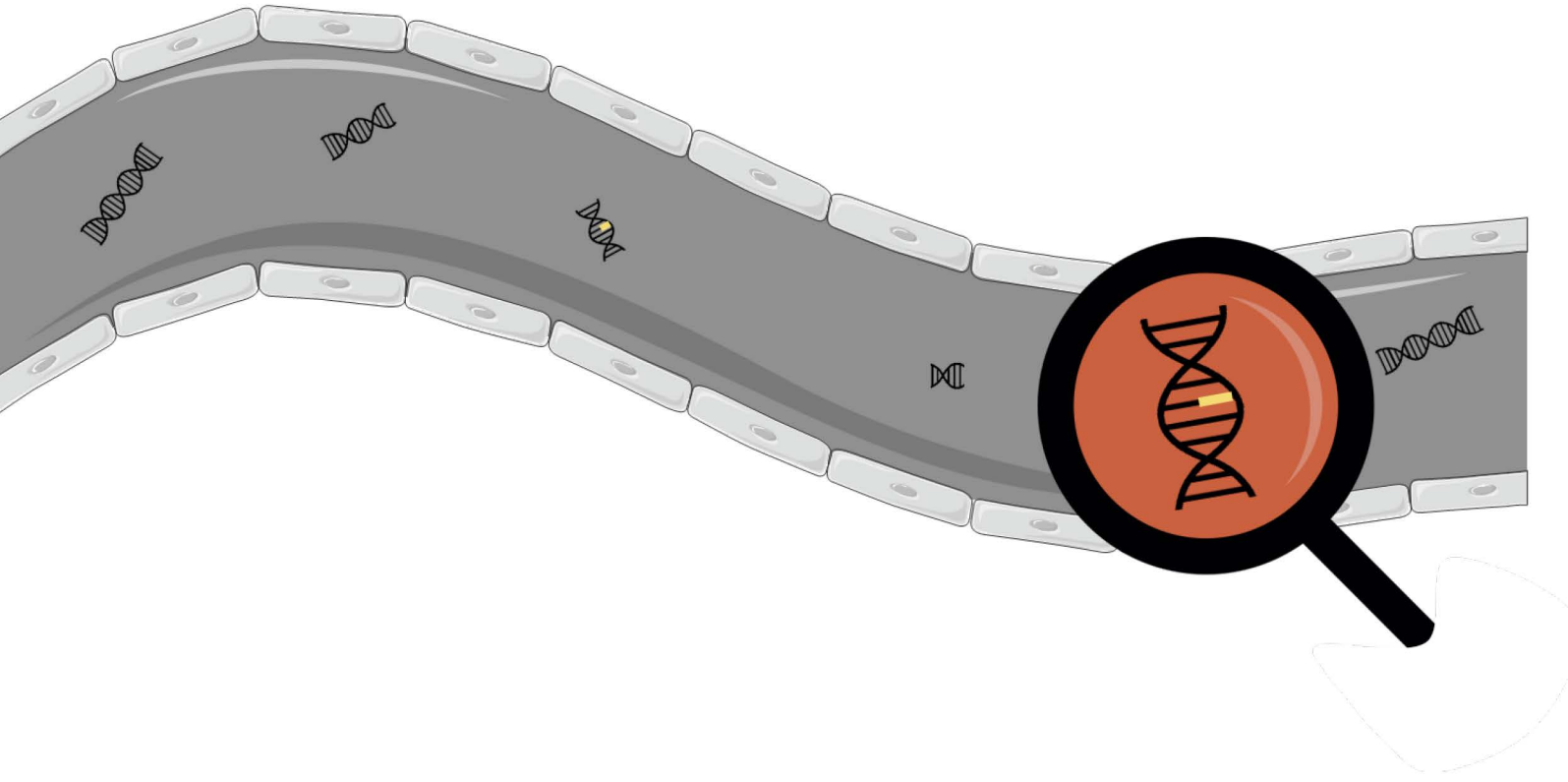

Joana Rita Fernandes Marques

Breaking the ctDNA sensitivity barrier

Tese de Mestrado em Biologia Celular e Molecular,
realizada sob a orientação científica do Professor Doutor José Luís Costa (Ipatimup/i3S, Universidade do Porto)
orientação interina da Professora Doutora Maria Carmen Alpoim (Departamento de Ciências da Vida, Faculdade de Ciências e Tecnologia, Universidade de Coimbra),
e apresentada ao Departamento de Ciências da Vida da Faculdade de Ciências e Tecnologia da Universidade de Coimbra (DCVFCTUC).

Setembro 2017

· U C ·

Universidade de Coimbra

Joana Rita Fernandes Marques

Breaking the ctDNA sensitivity barrier

Tese de Mestrado em Biologia Celular e Molecular, realizada sob a orientação científica do Professor Doutor José Luís Costa (Ipatimup/i3S, Universidade do Porto) e orientação interina da Professora Doutora Maria Carmen Alpoim (Departamento de Ciências da Vida, Faculdade de Ciências e Tecnologia, Universidade de Coimbra), e apresentada ao Departamento de Ciências da Vida da Faculdade de Ciências e Tecnologia da Universidade de Coimbra (DCV-FCTUC).

Setembro 2017

· U C ·

UNIVERSIDADE DE COIMBRA

ACKNOWLEDGMENTS

Em primeiro lugar gostaria de agradecer ao meu orientador Professor Doutor José Luís Costa pela disponibilidade e orientação científica sempre numa perspetiva desafiadora que me ajudou a dar os primeiros passos na ciência com a ambição de ir sempre mais além.

À minha co-orientadora Professora Doutora Maria Carmen Alpoim um agradecimento pela disponibilidade, aconselhamento e espirito crítico, que contribuíram para o enriquecimento deste trabalho.

Ao Professor Doutor José Carlos Machado pela oportunidade de realizar esta tese no grupo "Genetic Dynamics of Cancer Cells", no i3S-Instituto de Investigação e Inovação em Saúde, Universidade do Porto, e pela partilha de conhecimentos.

Ao patologista Doutor Jorge Pinheiro pela colaboração e partilha de conhecimento indispensáveis para a análise das amostras de tecido e respetiva interpretação dos resultados incluídos neste trabalho. I would like to express my gratitude to Dr. Alain Thierry for the kind offer and support which allowed me to perform an important task of my work.

Aos meus colegas de grupo um muito obrigado por me terem ajudado na realização deste trabalho, pelas caminhadas GEDY, pelo convívio, pelo apoio e boa disposição… Em particular à Joana e à Helena pela ajuda em certas técnicas laboratoriais, pela disponibilidade e pelos momentos partilhados. À Cecília pela ajuda na análise estatística dos resultados apresentados.

À Susana, minha grande companheira nesta etapa, por tudo o que me ensinaste, pelo apoio incondicional, pelos conselhos e pelo otimismo constante! És um exemplo para mim como colega e ainda mais como amiga pela tua honestidade e simpatia… deve ser do signo! Obrigada por acreditares em mim, por suportares o meu mau humor com muita paciência e por teres estado a meu lado quando precisei, sempre com as palavras certas. Obrigada pelas gargalhadas e todos os momentos partilhados.

Aos meus colegas de mestrado que partilharam comigo esta etapa. Um agradecimento especial à Catarina, Joana e Mariana pela partilha de momentos, pela presença e apoio constante e por me acompanharem na descoberta no mundo além-fronteiras.

Às sete melhores pessoas que Aveiro me deu, obrigada por estarem sempre presentes apesar da distância, pelos momentos e ensinamentos partilhados ao longo desta etapa. À Ana e Alexandra um agradecimento especial por terem sempre uma palavra de apoio e por me ajudarem sempre a olhar a vida de uma forma mais positiva.

Ao Ricardo, por ser um otimista incurável, por levar a vida com descontração e pelos cozinhados. Obrigada pela paciência, por estares sempre presente, por me ajudares a encarar cada desafio com um sorriso e por partilhares comigo este gosto pela ciência.

À minha família, especialmente aos meus pais e irmão um agradecimento muito especial por serem o meu grande apoio. Pelas palavras de alento e por estarem sempre a meu lado quando mais preciso, por me compreenderem e por sempre me terem incentivado a ser a melhor versão de mim mesma! Ao Tiago, por ter sido o meu motorista particular ao longo deste ano, pela companhia, pelas jantaradas e pelo apoio.

RELEVANT ABBREVIATIONS

ANX V	Annexin V
bp	Base pairs
cfDNA	Cell-free DNA
CT	Computed tomography
CTCs	Circulating tumor cells
ctDNA	Circulating tumor DNA
DAB	3, 3 –diaminobenzidine substrate
DMSO	Dimethyl Sulfoxide
DNA	Deoxyribonucleic acid
EGFR	Epidermal growth factor receptor gene
FBS	Fetal bovine serum
FDA	Food and Drug Association
FELASA	Federation for Laboratory Animal Science Associations
FISH	Fluorescence *in vitro* hybridization
FITC	Fluorescein isothiocycinate
IHC	Immunohystochemistry
KW	Kruskall Wallis test
MRI	Magnetic resonance imaging
MTT	3-(4,5-dimethylthiazol-2-yl)-2,5-diphenyltetrazolium-bromide
NaCl	Sodium chloride
NGS	Next generation sequencing
NSCLC	Non-small cell lung cancer
ON	Overnight
OS	Overall survival
PCR	Polymerase chain reaction
PE	R-phycoerythrin
PET	Positron emission tomography
PFS	Progression-free survival
PS	Phosphatidylserine
RNA	Ribonucleic acid
RT	Room temperature
SCLC	Small cells lung cancer
SD	Standard deviation
Spp.	species
TKIs	Tyrosine-kinase inhibitors
WHO	World health organization
WT	Wild-type

SUMMARY

Over the years, advances in the molecular and biological understanding of cancer has changed the paradigm of clinical practice from a systematic to a personalized and targeted therapeutic approach. However, an accurate molecular characterization of the tumor is only achieved through tissue biopsy, an invasive strategy that comprises many limitations. In this context, liquid biopsy, peripheral blood sample, comes as an alternative. Technological advances for detection and characterization of tumor-specific mutations in plasma have revealed its potential clinical relevance as biomarkers for tumor detection, response to therapy and disease follow-up. Despite the exciting breakthroughs, the intrinsic low abundance of circulating tumor DNA (ctDNA) makes the detection of such mutations in plasma a challenging task. This problem has been tackled by the development of high sensitive technologies but their complexity makes them difficult to implement in clinical routine. In alternative, our hypothesis was that pre-treatment of patients with cytotoxic drugs could increase the levels of ctDNA allowing the use of routine methodologies for the detection of tumor derived mutations in plasma. The major goal of this study was to test the effect of cytotoxic chemotherapeutic drug treatment on the levels of ctDNA. More specifically, we aimed to determine the effective therapeutic concentration with effect on ctDNA release and the ideal time point for blood collection after treatment.

In order to address our hypothesis, i*n vitro* assays were performed in lung cancer cell lines to establish the dose and time dependent effect of widely used cytotoxic chemotherapeutics. Liquid biopsies strategies were adopted to assess the effect of single drug treatment in DNA release levels both i*n vitro* and *in vivo* using xenografted mice models. Additionally, identification of ctDNA was achieved through the detection of specific sequences of DNA derived from the plasma of xenografted mice.

The results have shown that docetaxel was the most effective drug to reduce cell viability. This effect correlated to significant increase levels of late apoptosis in cells 48h after treatment with docetaxel. Additionally, *in vitro* drug treatment induced an increase in ctDNA release levels, with a greater effect at the 48h time point, suggesting an impact of docetaxel in cfDNA release. *In vivo*, a single dose treatment of docetaxel (25 mg/Kg) resulted on increased tumor apoptosis at 48h which correlates with increased levels of cfDNA detected in plasma. The specific detection of increased levels of tumor-derived DNA confirmed the influence of docetaxel treatment on

ctDNA release. Furthermore, xenograft mice treated with docetaxel revealed increased mutational load when compared to untreated conditions, where the mutation was not detected.

Despite preliminary, these findings provide evidence that a single treatment with docetaxel approximately 48h prior to liquid biopsy, *in vivo*, can contribute to higher levels of ctDNA and consequently overcome the problem of low sensitivity of detection. Moreover, the present work indicate apoptosis as the major release mechanism of ctDNA. Altogether, this study provided new insights into a novel strategy which might accelerate the implementation of ctDNA detection as a liquid biopsy strategy on the clinical routine and have an impact on clinical management of patients.

RESUMO

O estudo da biologia molecular do cancro tem permitido avanços científicos com impacto na prática clínica, mudando o paradigma de abordagem terapêutica convencional, sistémica, para uma abordagem personalizada. No entanto, a caracterização molecular de tumores sólidos só é possível através da biopsia do tecido, uma estratégia altamente invasiva com diversos riscos e limitações associadas. Neste contexto, a biopsia líquida, colheita de sangue, surge como uma alternativa. Avanços tecnológicos para deteção e caracterização de mutações específicas do tumor presentes no plasma permitiram a descoberta da relevância clínica do ADN circulante como biomarcador no diagnóstico, resposta a terapia e monitorização da doença. Apesar destas descobertas, a baixa abundância do ADN tumoral em circulação torna difícil a deteção de mutações relevantes. Estratégias para a resolução deste problema incluem o desenvolvimento de novas metodologias, mais sensíveis, para a deteção de mutações raras. No entanto estas estratégias são ainda muito complexas e dispendiosas para serem aplicadas na prática clínica. Assim, a nossa hipótese é que o pré-tratamento dos pacientes com quimioterápicos poderá aumentar os níveis de ADN tumoral em circulação permitindo o uso das metodologias disponíveis para deteção, no plasma, de mutações derivadas do tumor. O principal objetivo desta dissertação foi testar o efeito do uso de quimioterápicos nos níveis de ADN tumoral circulante de forma a ultrapassar a baixa sensibilidade de deteção das metodologias disponíveis na clínica. Especificamente, determinamos a dose terapêutica efetiva com impacto nos níveis de ADN circulante e o momento ideal para realização da biopsia líquida após tratamento de forma a maximizar a deteção de ADN tumoral circulante.

Foram realizados ensaios em linhas celulares de cancro do pulmão de forma a determinar o efeito da concentração e do tempo do tratamento com quimioterápicos usados na prática clínica. De modo a determinar o efeito do tratamento com docetaxel na libertação de ADN circulante, estratégias de biopsia líquida foram aplicadas tanto *in vitro* como *in vivo*. Por fim, a deteção de ADN tumoral circulante foi feita com a utilização de sondas específicas para sequências de interesse do ADN tumoral.

Verificámos que o docetaxel foi o quimioterápico mais eficiente a reduzir a viabilidade celular, o que foi concordante com o aumento dos níveis de apoptose verificados 48h após tratamento. Os níveis aumentados de ADN circulante, observados *in vitro*, após 48h de exposição ao docetaxel, sugerem o impacto do tratamento nos níveis de apoptose e consequentemente na

quantidade de ADN circulante. *In vivo*, o tratamento com uma dose de docetaxel (25 mg/Kg) provocou o aumento dos níveis de apoptose 48h após tratamento, um aumento que também se verificou relativamente aos níveis de ADN circulante. Especificamente, foi possível detetar níveis aumentados de ADN proveniente do tumor no plasma de ratinhos tratados com docetaxel, quando comparado com ratinhos não tratados. Foi detetado um aumento na sensibilidade de deteção da mutação específicas do tumor no plasma de ratinhos após tratamento com docetaxel, o que não se verificou para os animais não tratados.

Este estudo apresenta evidências preliminares de que uma dose única de docetaxel 48h antes da realização de biopsia líquida, *in vivo*, pode contribuir para o aumento dos níveis de ADN em circulação e consequentemente, ultrapassar o problema de sensibilidade de deteção de mutações raras. Neste estudo também foi possível verificar a importância do processo de apoptose como um mecanismo de libertação de ADN tumoral. Esta estratégia inovadora poderá agilizar a aplicação da deteção de ADN circulante (biopsia líquida) como biomarcador, na prática clínica, para a monitorização do cancro.

TABLE OF CONTENTS

FIGURE INDEX

TABLE INDEX

1. INTRODUCTION

1.1. CANCER

Cancer is known as a genetic disease characterized by a wide range of genetic and epigenetic alterations (1,2). External environmental factors, such as exposure to mutagens and viruses, and the hereditary component, inherited genetic variations, can contribute to carcinogenesis. Besides this factors, DNA replication errors occurring during division of normal stem cells, seems to be a major contributor to carcinogenesis (3). During normal cell division a significant number of mutations are introduced in the DNA sequence but the majority of these mutations can be effectively repaired by DNA damage repair mechanism (1,4). Cells that fail to be repaired are programmed to undergo growth-inhibitory processes, either apoptosis, differentiation or senescence which keep a low rate of mutations in normal cells (5). The remaining mutations can be referred as "passengers" once they accumulate in normal cells but have no effect on neoplastic process (6). Nevertheless, accumulation of stochastic somatic cell mutations can lead to alterations in a few specific genes, "driver" genes, which regulate key pathways of cell proliferation, cell survival and apoptosis (5). These "driver" genes, oncogenes and tumor suppressors genes, have been described as genes containing "driver" mutations that are likely to eliminate the balance between cell proliferation and cell death, resulting in increased activity of cell growth pathways while suppressing apoptotic mechanisms, conferring a selective growth advantage to cells that promote tumorigenesis (6).

Tumor evolution can culminate in metastasis formation, tumor mass formation far from the primary tumor localization, due to invasive capacity of the tumor cells which may disseminate via lymphatic or blood systems (7). The constant evolution of cancer genetics represent a challenge for cancer management and therapeutic decision (10).

Tumors are complex systems where microenvironment, consisting of many different cell types and supporting structures, interact with tumor cells and influence tumor growth and dynamics (10). The study of all these players in tumor evolution is difficult due to its high complexity but new insights have been given through recent technologic advances based on high-throughput and systematic profiling of cancer at different levels, namely at genomic level (1).

Regarding epidemiology, cancer is considered a prominent cause of death with approximately 14.1 million new cancer cases and 8.2 million cancer deaths worldwide in 2012 (11,12). Overall, lung, breast and colorectal cancer have the highest incidence rate, in both genders (Figure 1 (A))

(12,13). Lung, stomach and liver cancers comprise the higher mortality rates worldwide (Figure 1 (B)) (11,13). In Portugal, colorectal, lung and stomach cancers occupy the top 3 with higher mortality rate (Figure 1 (C)) (13). Over the years, increased incidence is in part justified by population growth, aging and risk lifestyle behavior including smoking, overweight and physical inactivity (11). This data highlight the importance of cancer research in order to better understand the biology of this disease and develop new and more effective strategies for diagnosis and therapy.

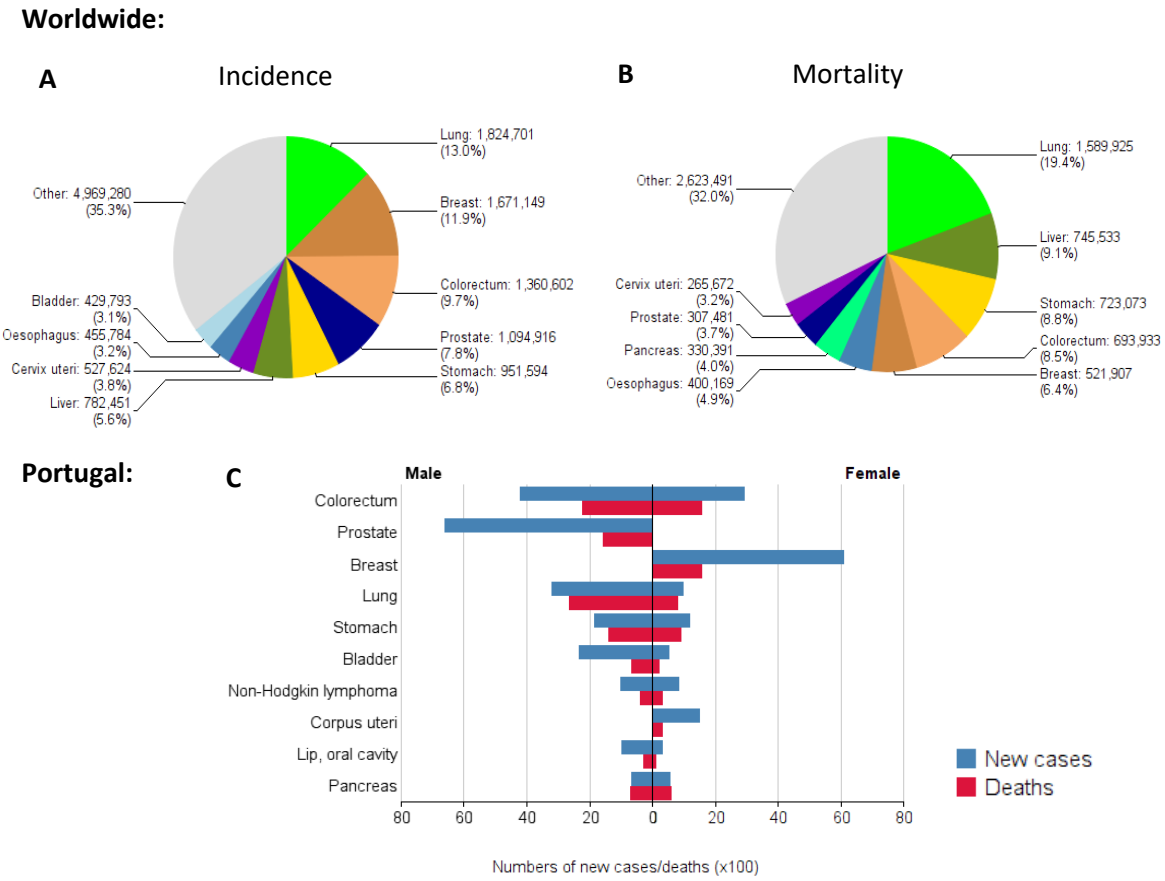

Figure 2. Cancer statistics. Incidence and mortality of several cancer types worldwide (A, B) and in Portugal (C). Adapted from (13).

1.1.1. Lung Cancer

Lung cancer is the most frequently diagnosed cancer and the one with higher mortality in man worldwide (Figure 1 (A,B)) (11). The main risk factors for lung carcinogenesis are smoking and use of tobacco products, other lifestyle behaviors of risk include exposure to radon gas, asbestos, air pollution and chronic infections (14).

Lung cancer can be divided in two main classes: small-cell lung cancer (SCLC) and non-small cell lung cancer (NSCLC) (15). NSCLC represent 85% of the total cases of lung cancer and it can be subdivided based on immunohistological classification in three main subtypes: squamous cell lung cancers, adenocarcinomas and large cell anaplastic carcinomas (14,15). Subtypes characterization is presented in Table 1. The World Health Organization (WHO) has recently summarized some alterations in classification of lung cancer due to advances in lung cancer genetics and therapy since 2004 (16). This classification is of great importance to guide clinical decisions and therapeutic strategies (17). Besides histologic classification, lung cancer patients are stratified using de TNM system, an international TNM-based staging system that describes the anatomical features of primary tumor size and burden (T), lymph nodes involvement (N) and presence of distant metastasis (M) (14,18). Each anatomical feature uses a numeric scale to describe the extent of cancer (14,18). Compilation of these features allow stratification of patients in staging groups, from I to IV, that guide clinicians in therapeutic decision, prognosis and help evaluation of response to treatment. Due to the late symptomatology of lung cancer, the majority of patients are diagnosed in an advanced stage of disease (14,19).

Table 2. Characterization of lung cancer subtypes. Adapted from (14).

Lung Cancer Type	% of all lung cancer	Anatomic location
Squamous cell lung cancer	25-30%	Main bronchi
Adenocarcinoma	40%	Peripheral bronchi
Large cell anaplastic carcinoma	10%	-
Small cell lung cancer	10-15%	Hormonal cells of the lung

Lung cancer has been described to have one of the highest somatic mutation rates (an average of 147 non-synonymous mutations for NSCLC) which are normally associated with interference of a potent mutagen (6). Recent advances in technology have increased the understanding of lung cancer features and complexity in terms of genomic alterations through development of more sensitive strategies such as genome-wide sequencing (15). Molecular profiling of various lung adenocarcinomas permitted the identification of different genomic alterations that comprise non-synonymous point mutations or splicing site alterations, rearrangement through modification of nucleotide ring structure, somatic copy number variation and fusion mechanisms (20). It has also been shown that there are specific genetic alterations for each of the major histological subtypes of lung cancer (21). Furthermore, genetic profiling has helped the identification of alterations in genes, more specifically oncogenes including *KRAS*[1], *EGFR*[2],

[1] KRAS proto-oncogene
[2] Epidermal growth factor receptor

BRAF[3], *PI3KCA*[4] and *ERBB2*[5]. Some tumor suppressor genes also appear to be inactivated namely *TP53*[6], *RB1*[7], *CDKN2A*[8] and *PTEN*[9] (14,22,23). Rearrangements in *ALK*[10], *ROS1*[11], *RET*[12] and *NTRK1*[13] have also been described in lung carcinogenesis. From these genes, activation of the proto-oncogene *EGFR* is one of the most common alterations among NSCLC patients which together with KRAS and ALK constitute relevant targets for clinical practice and therapeutic approaches (15,21–23).

Diagnosis methodologies for lung cancer can be subdivided into non-invasive, imaging procedures, and invasive sampling strategies. Non-invasive strategies include computed tomography (CT), Positron Emission Tomography (PET), Magnetic Resonance Imaging (MRI), or Positron Emission Tomography PET-CT inspection (24,25). These strategies allow the detection of suspicious nodes with potential malignancy and their specific localization and extent. Unfortunately, this is not enough for definitive diagnosis which is only achieved through cytological, histological and molecular analysis dependent on invasive strategies, either surgical open biopsy, needle biopsy techniques or others (24,25). Molecular analysis can be obtain through fluorescence *in vitro* hybridization (FISH) or immunohistochemistry (IHC), for identification of specific molecular targets (18). Improvements in diagnostic strategies include the implementation of ultrasound-guided needle biopsy, bronchoscopy biopsy, etc. In lung cancer, lung positioning within the thoracic cavity make tumor tissue collection a challenging task (28). To avoid lung biopsy, metastatic lung cancer patients can be diagnosed based on metastatic tissue analysis, however this sample is not fully representative of the primary tumor, mainly in what concerns to molecular profiling (28).

Lung cancer treatment is highly dependent on stage of disease. For early stages (I, II and III) the primary option for localized tumor mass is surgery which is correlated with best long-term survival (27). In unresectable tumors, adjuvant platinum-based chemotherapy, radiotherapy or both in simultaneous are currently used (29,30). At stage IV, advanced metastatic NSCLC patients have a low 5 years survival where palliative treatment, such as external radiation

[3] B-Raf proto-oncogene
[4] Phosphatidylinositol-4,5-biphosphate 3-kinase catalytic subunit alpha
[5] Erb-b2 receptor tyrosine kinase
[6] Tumor protein P53
[7] Retinoblastoma transcriptional corepressor 1
[8] Cyclin dependent kinase inhibitor 2A
[9] Phosphatase and tensin homolog
[10] ALK receptor tyrosine kinase
[11] ROS proto-oncogene 1
[12] Ret proto-oncogene
[13] Neurotrophic tyrosine kinase, receptor type 1

therapy or surgery, can be a suitable option to attenuate symptoms (27,31). Unfortunately, the majority of NSCLC patients are diagnosed at this stage where surgery is no longer a viable option due to increased extent of the tumor and metastasis formation (14,32). If molecular analysis are not available first-line chemotherapy including platinum-based chemotherapeutics, cisplatin or carboplatin, can be used alone or in combination with other classes of chemotherapeutics to improve clinical outcome (14,29,33).

Based on molecular profiling of advanced NSCLC tumors, development of targeted and personalized therapies have been possible to implement in the clinic. For EGFR-mutation positive tumors, first-generation EGFR tyrosine kinase inhibitors (TKIs) can be used, namely erlotinib that has shown improved quality of life in comparison with standard chemotherapy (27,34). Another well-established molecular alteration is ALK rearrangement. ALK-positive NSCLC are sensitive to treatment with crizotinib, a TKI with promising results in improving survival of patients (14,27,35). Unfortunately, acquired resistance to targeted therapy have been observed in lung cancer patients. Nevertheless, some second and third-generation TKIs were already approved to target the resistance mutations in EGFR mutated patients (17,36). ALK positive patients can also develop resistance that can be overcome with new-generation ALK inhibitors (29,37). Immunotherapy is also an emerging field of therapeutic options that targets the immune system trying to reverse the immunosuppressive environment of tumor. Immune checkpoint inhibitors and vaccine therapies are some of the strategies that are being used to improve treatment response in NSCLC patients (14,38–40).

In general, an accurate diagnosis comprises many limitations associated with invasive methodologies used for tissue collection that represent discomfort and risk for the patient and require specialized technicians (22). Furthermore, the amount of biopsy material can be insufficient for histologic and molecular analysis and the small fragments collected may not be representative of tumor genetics (9,41–43). Regarding treatment, advances in molecular and biological understanding of cancer is changing the paradigm from a systematic treatment to a personalized and targeted therapeutic approach, the era of personalized medicine (44,45). Unfortunately, the use of personalized approaches has shown, in some patients, development of resistance, a problem that is difficult to assess through tissue biopsy owing to the invasive character of this methodology, representing a challenge for targeted therapies application (46). The problematic of tumor heterogeneity have a great impact in this context since subpopulations with low representation in the tissue, at diagnosis, present an enrichment in the re-biopsy after loss of response to treatment (figure 3) (47). In fact, multiregional molecular

analysis of a tissue have shown an average of 70 somatic mutations, 55% of all mutations detected in the tumor (29,37). Moreover, only 34% of all mutations identified were present in all regions collected for analysis (48).

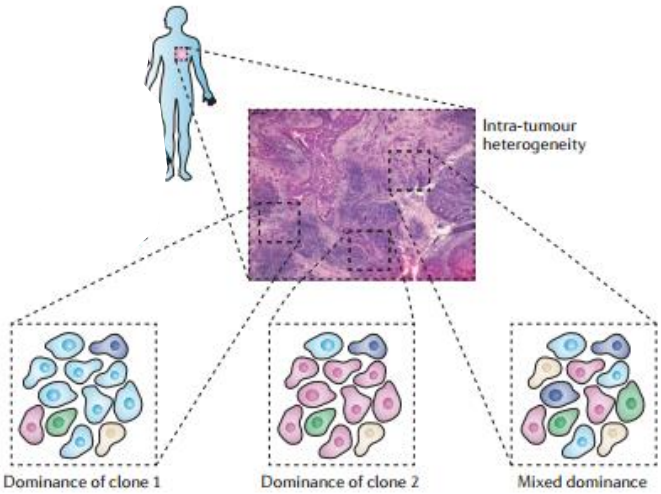

Figure 2. Intra-tumor heterogeneity of tumor tissue collected at diagnosis. Different subclones (genetically different) have a heterogeneous distribution in the tumor tissue. As a consequence, collection of a small fraction of the tumor may represent a problem for genetic characterization at diagnosis since a specific subclone may be more represented then other or may not even be present in the tissue collected. Adapted from (9).

1.2. LIQUID BIOPSY

Recently, there has been a focus on the need of novel, more comprehensive and less invasive biomarkers clinically relevant in diagnosis, prognosis and monitoring of cancer as a consequence of the new era of personalized medicine (45). Since tissue biopsy is an invasive method comprising many limitations, development of alternative sensitive methods, such as next generation sequencing (NGS), to detect reliable tumor-derived biomarkers may allow tumor characterization at diagnosis and over time (43,49). Detection of these biomarkers in body fluids, namely blood, is a less invasive strategy known as liquid biopsy, to oppose to the tissue/solid biopsy (50). Blood include many components beyond the characteristic hematopoietic cells. Detection of circulating nucleic acids (DNA and RNA) and exosomes in the plasma compartment and circulating tumor cells (CTCs) found in the cells compartment can be derived from the tumor mass and reflect cancer genome and tumor dynamics (figure 3) (51).

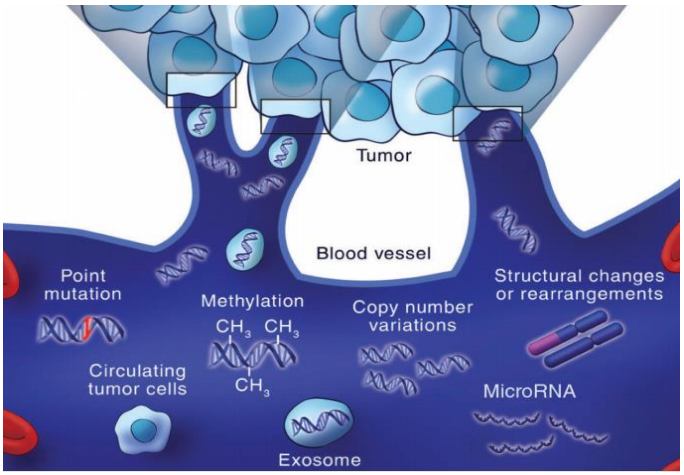

Figure 3. Tumor-derived components present in peripheral blood. Tumor material may be released into circulation as cells (CTCs), exosomes, DNA fragments and RNA. Adapted from (51).

1.2.1. Circulating tumor DNA

The discovery of circulating nucleic acids, namely circulating free DNA (cfDNA), in peripheral blood date back to the late 40s when Mendel and Métais (52), first identified cfDNA in peripheral blood of healthy individuals, pregnant women and clinical patients. After this finding, only in 1977 new publications emerged on this topic. Leo et al (53), applied the study of circulating nucleic acids to oncology being the first to describe an increased concentration of cfDNA in cancer patients compared to healthy individuals. Over the years, the interest on detection of circulating tumor DNA (ctDNA) in plasma of cancer patients has expanded to study biology, new methodologies and potential application in the clinic.

The concept of ctDNA refers to the presence of single- or double-stranded tumor DNA in circulation (54). These fragments of DNA are an instant picture of the tumor, representative of tumor genetics because it can include single-nucleotide mutations and epigenetic alterations also present in primary tumor cells (55). CtDNA has a short half-life in bloodstream ranging from 4 to 30 minutes (56). After collection, some biological characteristics of ctDNA are still unknown. For example, fragmentation and origin of cfDNA is still a topic of discussion. In a recent study, Jiang *et al.* (57), performed a detailed analysis of the size of ctDNA and concluded that ctDNA contains about 167 base pairs (bp), corresponding to the length of DNA in a chromatosome [nucleosome + linker histone] (58). Also, Thierry *et al.* (59), have demonstrated, for the first time, the presence of ctDNA with less than 100bp in plasma of cancer patients and that the proportion of DNA with fragment size of 150-400bp is highly related to non-tumor cfDNA rather than ctDNA.

In addition, both studies state that cfDNA from cancer patients is more fragmented than cfDNA present in healthy individuals (57,59). The characterization of the size of ctDNA is of extremely importance because it can give insights on its origin (60). The results obtained by Jiang *et al.* (57) suggest that these small fragments are derived from apoptotic tumor cells. In fact, fragment size distribution of apoptotic DNA include fragments of 166 bp (chromatosome unit), commonly referred as nucleosomes, and multiples units of a chromatosomes (185-200 bp), a pattern that has already been described in cancer patients (Figure 4 (B)) (61). The presence of bigger DNA fragments in circulation can indicate another origin, probably tumor cells necrosis. Nevertheless, apoptotic/necrotic non-tumor cells can also release nucleic acids into the blood, which dilute the pool of tumor-derived DNA in peripheral blood (Figure 4 (A))(45,62). Secretion of DNA from living tumor cells or CTCs is also an hypothesis under study to explain the presence of cfDNA in circulation (63). In the context of cancer it would be important to assess the tissue of origin of ctDNA released into circulation, to distinguish from the non-tumor cfDNA derived, for example, from lymphoid and myeloid cell types also present in healthy individuals and guide detection of tumor sites not detected in imaging analysis. Recent studies in epigenetics have demonstrated that the circulating DNA is nucleosome-protected DNA and affirmed that nucleosome footprint of protein-DNA interaction, cfDNA nucleosome fragmentation patterns and methylation patterns in cfDNA can indicate the cell type of origin of the ctDNA in cancer patients (60). Since the discovery of ctDNA in cancer patients it is accepted that an increased concentration of DNA in plasma is observed when compared to healthy individuals. However, the precise ctDNA concentration is still undetermined since it is very variable between cancer patients (62). Despite variable, the amount of ctDNA often corresponds to a small fraction of total cfDNA (down to <0.01 %) (64,65). Regarding this limitation, Underhill *et al.* (66), demonstrated that selection of shorter fragments of cell-free DNA (20-30bp shorter than healthy cell-free DNA) may improve sensitivity of ctDNA detection in circulation.

1.2.2. Applications and limitations

The study of nucleic acids in circulation in pathological conditions, in particular cancer, have revealed great potential on their application in the clinic for early diagnosis, patient stratification, monitoring of disease progression and response to therapy, namely efficacy and resistance mechanisms. Unfortunately, almost all these applications are still in an experimental level due to the absence of standard sensitive methods for biomarkers detection in cancer and the poor understanding of the biology and dynamics of these biomarkers. Besides the use of

fetal cfDNA in clinic for pre-natal genetic diagnosis and testing, the application of cfDNA detection in cancer is now giving the first steps into the clinic (43,67).

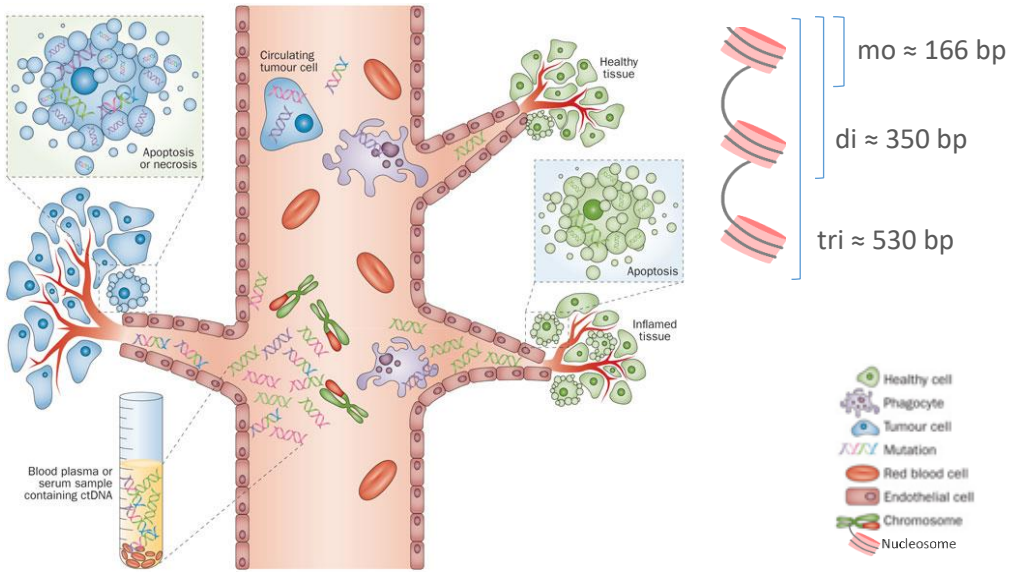

Figure 4. Properties and origin of cfDNA. (A) DNA in circulation can be derived from tumor or healthy cells through apoptotic or necrotic processes. CtDNA contains mutations representative of tumor genetics and may be extracted from the plasma of patients. (B) Pattern of fragmentation of DNA from apoptotic origin corresponding to a mononucleosome (mo), dinucleosome (di) and trinucleosome (tri). Core histone (pink) and DNA (grey line). Adapted from (45).

Several studies have reported a significant increase on ctDNA in patients with different cancer types, namely breast, colorectal and NSCLC, when compared to healthy individuals (68–70). This represent a possible application for ctDNA in early diagnosis, as an alternative of the invasive tissue biopsy (71). Nevertheless, the amount of cfDNA cannot be used alone as a diagnostic tool due to limitations related to the small fraction of ctDNA in circulation, the proportion of asymptomatic patients with detectable ctDNA, for example (68,72). The addition of genetic characterization of ctDNA may improve the value of this biomarker at diagnosis (42,68,70). The genetic alterations present in the ctDNA can reveal tumor heterogeneity. The "scanning" of cancer genome in plasma have allowed the identification of point mutation, copy number aberrations and chromosomal alterations (73). For instance, in lung cancer patients it has been demonstrated that cancer cells carry several types of activating EGFR mutations simultaneously which are also detectable in circulation, even before starting targeted therapy treatments (74).

The study of ctDNA in peripheral blood is a promising biomarker for monitoring tumor progression. ctDNA is highly sensitive and representative of tumor genetics as demonstrated by

F. Imamura *et al* (74). The dominant mutation in ctDNA at disease progression was the same as the mutations detected in re-biopsy cancer patients, which make the identification of genetic profile of the tumor during disease progression a useful application for detection of ctDNA. Regarding cfDNA dynamics, high levels of cfDNA are associated with tumor volume and number of metastatic sites during tumor progression (75). In addition, correlation between changes in cfDNA levels and tumor burden has been described as a prognostic marker (76).

Regarding monitoring tumor response to treatment, it has been described a decline in cfDNA levels after successful treatment with therapy or tumor surgery. A rapid increase in ctDNA levels reveal disease progression as a consequence of poor response to treatment. Stable disease is reflected in plasma with the absence of mutation or low levels of cfDNA (51,77,78). Recent studies have demonstrated correlation between early ctDNA responses and radiologic responses to a targeted therapy showing that, in some cases, it is possible to predict treatment response in the course of therapy through the detection of ctDNA even after radiologic confirmation or symptomatic relapse of disease (74,79). This is highly relevant in cancer patients to detect early resistance to targeted therapy and guide therapeutic decision (80). Due to the short life span of ctDNA in circulation it is possible to assess the changes in ctDNA concentration in real time and draw conclusion on the treatment response or resistance mechanisms.

Presence of ctDNA in peripheral blood was shown to be sufficiently sensitive to detect minimal residual disease after surgical resection or disease dormancy, revealing its prognostic value (51,65). Patients who have detectable ctDNA in circulation after surgery generally relapse within 1 year (71). A study demonstrated that ctDNA levels had a strong prognostic value on progression-free survival (PFS) and overall survival (OS) (81). In lung cancer, increased levels of cfDNA have been associated with poor PFS and OS (82). ctDNA appeared to be a better prognostic marker than CTC count when combined analysis of tumor-specific mutations in ctDNA and CTCs was performed (81).

Blood processing methods are one of the critical methodologic steps for successful ctDNA analysis. Standard blood collection methods should be determined, such as the type of collection tube to be used, time of blood processing after collection and conditions of storage. In the majority of clinical trials, ethylenediaminetetraacetic acid (EDTA) containing tubes are being used to collect blood to avoid blood coagulation. CfDNA can be isolated either from plasma or serum. Studies have recommended the extraction of ctDNA from plasma due to less risk of "contamination" with DNA from normal cells present in blood during the process of extraction (71). To optimize the detection of cfDNA, plasma should be processed within an hour after collection, due to the short life span of cfDNA (83). CtDNA characterization requires one step of

isolation and other of detection. Current ctDNA isolation strategies are complex and expensive. Thus optimization of isolation methods are crucial (71). Many studies comparing efficiency of isolation kits for cfDNA demonstrated that different methods affect the yields and quality of cfDNA revealing the need of standardization in the workflow for cfDNA analysis (84–86). Recently more sensitive, simple and inexpensive isolation strategies are been tested to accelerate implementation of ctDNA detection in the clinic (87). For example, automated platforms for extraction of ctDNA are being implemented, such as the QIAamp circulating nucleic acid kit (Qiagen), the most used in many clinical trials (83). Another important step includes DNA quantification that gives information on the amount and quality of the isolated DNA and can also quantifies tumor-associated genetic mutations. These include spectrophotometric methods, fluorescent dyes, or quantitative PCR-based methods, based on different targets for measurements that can in some cases lead to biased results (71). Hence, standardization of quantification methods used for ctDNA are also required. At this point, biology of cfDNA may have a great impact on the accurate analysis of cfDNA. The high fragmentation profile of cfDNA may affect quantification using PCR-based methodologies since these strategies rely mostly on the use of amplicons >100bp, missing smaller fragments of DNA, probably derived from the tumor (59). Initially, Sanger sequencing methodologies were available to detect somatic variations in tumor DNA but the low sensitivity of this approach made the application to ctDNA a challenging task (51). Thus, the need to develop new, more sensitive approaches.

The evolution of methodologies for ctDNA detection in terms of sensitivity are summarized in Table 2. Over the last years enormous advances have been achieved with NGS for DNA quantification and characterization. Today, single-nucleotide mutations in ctDNA may be detected through BEAMing, CAPP-seq, Safe-SeqS, TamSeq, and digital PCR (65,71,75,88,89). These are targeted approaches that aim to identify mutations in target genes, for example, EGFR or KRAS genes known to be potentially altered in lung cancer (90). These methodologies allow a detection of rare ctDNA mutation with an allelic fraction $\leq$ 0,01% (51,71). In the other hand, untargeted approaches, namely whole-genome sequencing or exome sequencing, allow a wide screening of the genome to identify unknown genomic alterations, such as driver mutations, mutations involved in resistance to targeted therapies (19,40), or a range of specific genes already characterized for specific cancer types down to an allelic frequency of 1-2% (71,91,92). It was recently developed a new panel including relevant mutated genes in NSCLC, gastrointestinal stromal tumor, colorectal carcinoma and melanoma (93). Targeted approaches have demonstrated a higher sensitivity, about 90%, when compared to untargeted approaches

with approximately 80% (71,94). For example, CAPP-Seq method for ctDNA quantification and analysis demonstrated 96% specificity for mutant allele fractions down to 0.02% (75).

Table 2. Methodologies for ctDNA detection. Adapted from (51).

Technique	Sensitivity	Application
Sanger sequencing	>10%	Tumor tissue
Next Generation Sequencing	2%	Tumor tissue
Quantitative PCR	1%	Tumor tissue
BEAMing, digital PCR, TAM-Seq, CAPP-Seq	≈0.01%	cfDNA, rare variants in tumor tissue

Beside the need of standardization, another barrier to the application of liquid biopsy strategies in the clinic is related to low abundance of ctDNA in circulation (95). The suboptimal sensitivity of ≈80% is being tackled through technological advances already mentioned. Regardless of the efforts to improve analytical strategies, these methods are still too expensive and complex to apply in the clinic. Recently, Thierry *et al.* (64) have developed the first multiplexed test for cfDNA using an allele-specific-Q-PCR-based method which allow a comprehensive characterization of cfDNA, from cfDNA quantification to the detection of a known point mutation and even the identification of the portion of tumor-derived DNA. Furthermore, highly sensitive and inexpensive methods based on nanopore technology are being developed to accelerate application of ctDNA detection in clinic routine (96). In 2014, European Medicines Agency (EMA) was the first to approve the application of a blood based diagnostic tool for the assessment of EGFR mutation status in those patients where a tumor sample is not an option (*therascreen* EGFR Plasma RGQ PCR kit, Qiagen) (97). In 2016, a platform for clinical application of cfDNA in EGFR mutation analysis was approved by Food and Drugs Administration (FDA) for NSCLC patients ("cobas EGFR Mutation Test v2", Roche), indicating the emerging applicability of cfDNA as a tool for cancer management (43)(98). Nevertheless an intensive effort is needed to harmonize liquid biopsy analysis workflow.

Overall, the analysis of ctDNA dynamics is revealing the potential of liquid biopsy relatively to conventional tissue biopsy since the use of ctDNA as a liquid biopsy strategy, can give a more representative characterization of the whole tumor genetics and allow sequential sampling for follow up of tumor progression, response to treatment, metastasis and disease recurrence. In fact, combination of the initial tissue collected at diagnosis with sequential liquid biopsy analysis

may give a more realistic monitoring of cancer progression and increase the reliability of the application of liquid biopsy in clinical routine (Figure 5).

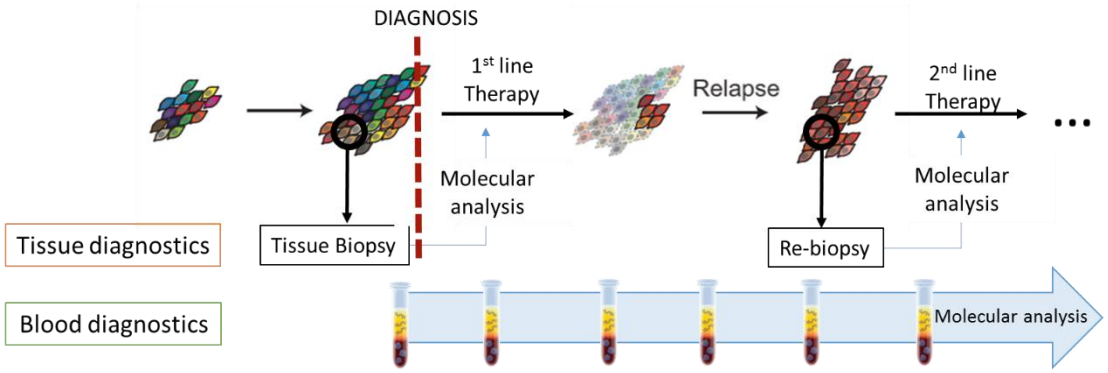

Figure 5. Guidance of cancer management using either tissue biopsy collection or serial liquid biopsy analysis. At diagnosis, molecular analysis are performed from the tissue collected to guide therapeutic decision, however in case of tumor relapse a re-biopsy is required to reevaluate the tumor landscape. The liquid biopsy allow a continuous evaluation of the tumor evolution through multiple blood sampling, which may help to guide therapeutic decisions.

2. AIMS OF THE STUDY

The interest on the use of ctDNA as liquid biopsy has widely increased in the scientific community during the last few years mainly due to technological advances for detection and characterization of this tumor biomarker and its potential clinical relevance. The major challenges delaying the introduction of liquid biopsy in the clinic routine are the low abundance of ctDNA and the lack of standard and highly sensitive methodologies for detection of quantifiable and high quality ctDNA. In this context, a more comprehensive knowledge of cfDNA biology and dynamics may help to overcome low abundance of ctDNA. Our proposal aims to address the low abundance of ctDNA from a different perspective, upstream of the detection technologies. As for many clinical procedures the patients have to be prepared before intervention, we suggest that patients might also be prepared before blood collection. Therefore, the major goal of this study was to test the effect of cytotoxic drug treatment on the levels of cfDNA in circulation as a mean to increase the level of ctDNA in circulation and overcome the low sensitivity of detection of available methodologies.

The specific aims of the study were:

- ✓ To determine the therapeutic concentration with effect on ctDNA release.
- ✓ To assess the ideal time point for blood collection after treatment.
- ✓ To identify the fraction of ctDNA within total circulating DNA.

In order to address our hypothesis, a drug screening was performed in several lung cancer cell lines harboring relevant mutations, to test the minimal effective drug concentration that affect viability of cells. The drugs selected were all cytotoxic chemotherapy drugs of different categories, namely docetaxel, gemcitabine and carboplatin. Time dependent effect of docetaxel was assessed through evaluation of cell apoptosis. *In vitro*, liquid biopsy strategy was adopted to assess the effect of drug treatment in DNA release levels. With the same purpose, liquid biopsy was performed in C57BL/6-*Rag2*$^{-/-}$ *IL2rg*$^{-/-}$ mice model xenografted with H1975 cells. In parallel, H1975 cells-derived tumors were analyzed for the impact of docetaxel treatment in proliferation and apoptosis. Selective identification of tumor derived DNA was achieved through detection of specific sequences of H1975 cells-derived tumor DNA present in plasma.

3. MATERIAL AND METHODS

The high incidence of lung cancer and the difficulties associated with lung biopsies makes this disease a prime model to develop this study. This project included *in vivo* experiments that required mice handling. For this propose, an introductory course in laboratory animal science was attended at the Institute for Molecular and Cell Biology, following FELASA category B recommendations.

3.1. BIOLOGICAL MATERIAL

3.1.1. CELL LINES

Three human lung adenocarcinoma cell lines were included in this study: HCC827, H1975 and A549 [ATCC – American Type Culture Collection, Lockville, MD, USA]. All the cell lines contain relevant mutations in genes involved in human lung adenocarcinoma (Table 3).

Table 3. Relevant genetic alterations in lung cancer cell lines.

Cell line	Gene	DNA change	Amino-acid change
HCC827	*EGFR*	c.2236_2250del15	p.E746_A750del
NCI-H1975	*EGFR*	c.2369C>T	p.T790M
		c.2573T>G	p.L858R
A549	*KRAS*	c.34G>A	p.G12S

All cell lines were grown in recommended complete medium, RPMI 1640 medium [Biowest, Nuaillé, France] , supplemented with 10% heat inactivated Fetal Bovine Serum (FBS) [Biowest, Nuaillé, France], and 1% Penicillin-Streptomycin (P-S) [GIBCO®, Life Technologies, Carlsbad, CA, USA]. Cells were maintained under conventional cell culture conditions at 37°C, in a humidified atmosphere containing 5% CO_2. Cell lines were grown in adherent monolayer and were subcultured using Trypsin-EDTA [Sigma-Aldrich®, St. Louis, MO, USA] to harvest cells when necessary to obtain the desired number of cells for *in vitro* studies performed.

All lung cancer cell lines were tested for *Mycoplasma* spp. contamination by PCR using two primers specific for 16S RNA of *Mollicutes* (MGSO: 5`- TGC ACC ATG TGT CAC TCT GTT AAC CTC – 3` and GPO1: 5`- ACT CCT ACG GGA GGC AGC AGT A – 3) [IDT – Integrated DNA Technologies, Coralville, IA, USA].

3.1.2. Animal Models

In vivo studies were performed using the C57BL/6-*Rag2*$^{-/-}$ *IL2rg*$^{-/-}$ mice model [Jackson Laboratory, Bar Harbor, ME, USA], an immunodefficient mouse model depleted of B, T and natural killer (NK) cells from the immune system, a condition required for the sucessful development of subcutaneous xenografts with cells of human origin. All animals were housed in polycarbonate cages (two to six per cage) and kept on a 12 hour light/dark cycle. Food and water was given *ad libitum*. All studies were conducted in accordance with the Direção Geral de Alimentação e Veterinária (DGAV) guidelines for care and use of laboratory animals.

3.2. CHEMICAL MATERIAL

3.2.1. Drugs

The anti-cancer chemotherapy drugs included in the *in vitro* studies were gemcitabine [USP, Rockville, MD, USA], carboplatin [BioVision Inc., Milpitas, CA, USA] and docetaxel [Alfa Aesar, Haverhill, MA, USA]. The categories and mechanism of action of these drugs are summarized in Table 4. Gemcitabine and carboplatin stock solutions were prepared in NaCl 0.9% [B. Braun, Melsungen, Germany]. Docetaxel stock solution was prepared in tween 80 [Sigma-Aldrich®, St. Louis, MO, USA] and ethanol 100% (v/v) [AppliChem, Darmstadt, Germany] and further diluted in NaCl 0.9%. The drugs diluent was used as vehicle in all experiments performed.

Table 4. Characterization of anti-cancer chemotherapy drugs.

DRUG	CATEGORY	TARGET	RESULT
Carboplatin	Metal-based drug	DNA	Cell cycle arrest in S phase. Apoptosis or necrosis
Gemcitabine	Antimetabolite - pyrimidine analog	DNA synthesis	Cell cycle arrest in S phase. Apoptosis
Docetaxel	Anti-mitotic agent – (Taxanes)	Microtubules dynamics (stabilizer)	Cell cycle arrest during mitosis. Apoptosis

3.3. METHODS

3.3.1. CELL VIABILITY ASSAY

The effect of standard chemotherapy on viability of the three cell lines was indirectly evaluated using the 3-(4,5-dimethylthiazol-2-yl)-2,5-diphenyltetrazolium-bromide (MTT) assay. MTT is a yellow compound metabolized by viable cells forming formazan crystals, purple compound used to measure enzimatic activity of cells and indirectly their viability. Briefly, cells were seeded in 96-well plates [TPP®, Trasadingen, Switzerland], 5000 cells per well and incubated at 37ºC/5%CO_2. Cells were allowed to adhere and once 40%-60% confluence was reached cells were treated with the aforementionated drugs, at increased drug concentrations (Table 5). Control condition (no treatment) and vehicle condition (treatment with drugs' diluent) were also included in each experiment. Cells viability was measured by MTT assay at 24h, 48h and 72h after treatment. Medium was removed and cells were incubated with 15 µL of MTT solution (5mg/mL) [Sigma-Aldrich®, St. Louis, MO, USA] diluted in culture medium to a final concentration of 0.5 mg/mL, for 3h at 37ºC/5%CO_2. After incubation, MTT solution was removed and formazan crystals were dissolved using 100µL dimethylsulfoxide (DMSO) [Merck, Darmstadt, Germany]. Finnaly, plates were gently shaked to ensure total dissolution of the crystals and absorvance was measured at a wavelenght of 560 nm using a Synergy Mx microplate reader [BioTek, Winooski, VT, EUA]. Two independent experiments were performed with six replicates per condition.

Table 5. Drug concentration selected to test effect of treatment the viability of cells.

Drug name	Concentration (µM)
Carboplatin	0.01 < 0.1 < 1 < 10 < 100
Docetaxel	0.001 < 0.01 < 0.1 < 1 < 10
Gemcitabine	0.01 < 0.1 < 1 < 10 < 100

3.3.2. APOPTOSIS ASSAY – FLOW CYTOMETRY

The dose and time dependent effects of docetaxel and gemcitabine in H1975 cell line apoptosis was evaluated using the APOAlert™ annexin V-FITC Apoptosis Kit [Clontech Laboratories, Mountain View, CA, USA], according to manufacturer's instructions. This kit allows the study of apoptosis by detection of changes in phosphatidylserine levels (PS) present in cell membrane.

In non-apoptotic cells, most PS molecules are localized at the inner layer of the plasma membrane but in initial phases of apoptosis, PS translocate to the outer layer of the membrane. Annexin V (ANX V) is a protein with high affinity to PS that can be used to detect exposed PS and, consequently, cells undergoing early apoptosis. Propidium Iodide (PI) is a fluorescent intercalating agent that stains cells with permeable membranes, in a late stage of apoptosis. Briefly, H1975 cells were seeded in 6-well plates [TPP®, Trasadingen, Switzerland] at 350000 cells per well and incubated at 37ºC/5%CO_2. Cells were alllowed to adhere and once 40%-60% confluence was attained cells were treated with docetaxel (0.001 µM; 0.1 µM) and gemcitabine (0.01 µM and 1 µM). Apoptosis levels were measured after 12, 24h, 36h and 48h. At each time point, cells were harvest and the appropriate suspension volume transferred to a 96-well plate to obtain 100000 cells for each condition. Cells were incubated with a mixture containing 200 µL of binding buffer, 5 µL of Annexin V (FITC) and 10 µL of PI (PE) for 15 min, protected from light. After incubation, cells were transferred to FACS tubes [FALCON®, Corning Science, Tamaulipas, México] and analised by flow cytometry using BD FACSCanto™ II [BD Biosciences, San Jose, CA, USA] and FlowJo software [FlowJo® LLC, Ashland, OR, USA]. One independent experiment was performed with biological triplicates for each condition.

To perform flow cytometry analysis a gating strategy was defined in the FlowJo software as described in Figure 6. Briefly, cellular debris were excluded with the first gate and only single cells were selected with the second gate according to the area vs height of the cells. PE-A is the channel for PI signal detection and FITC-A channel detects annexin V signal. Based on this knowledge, unstained and monolabel conditions (cells stained only with annexin V or PI) were used to define quadrants for apoptosis analysis. All channels were compensated to ensure that only the channels for PI and annexin V signal were being used. Q1 refers to viable cells (PI^-ANX V^-), Q2 contain cells at an early stage of apoptosis (PI^-ANX V^+), Q3 cells in late apoptosis (PI^+ANX V^+) and Q4 represents death cells (PI^+ANX V^-).

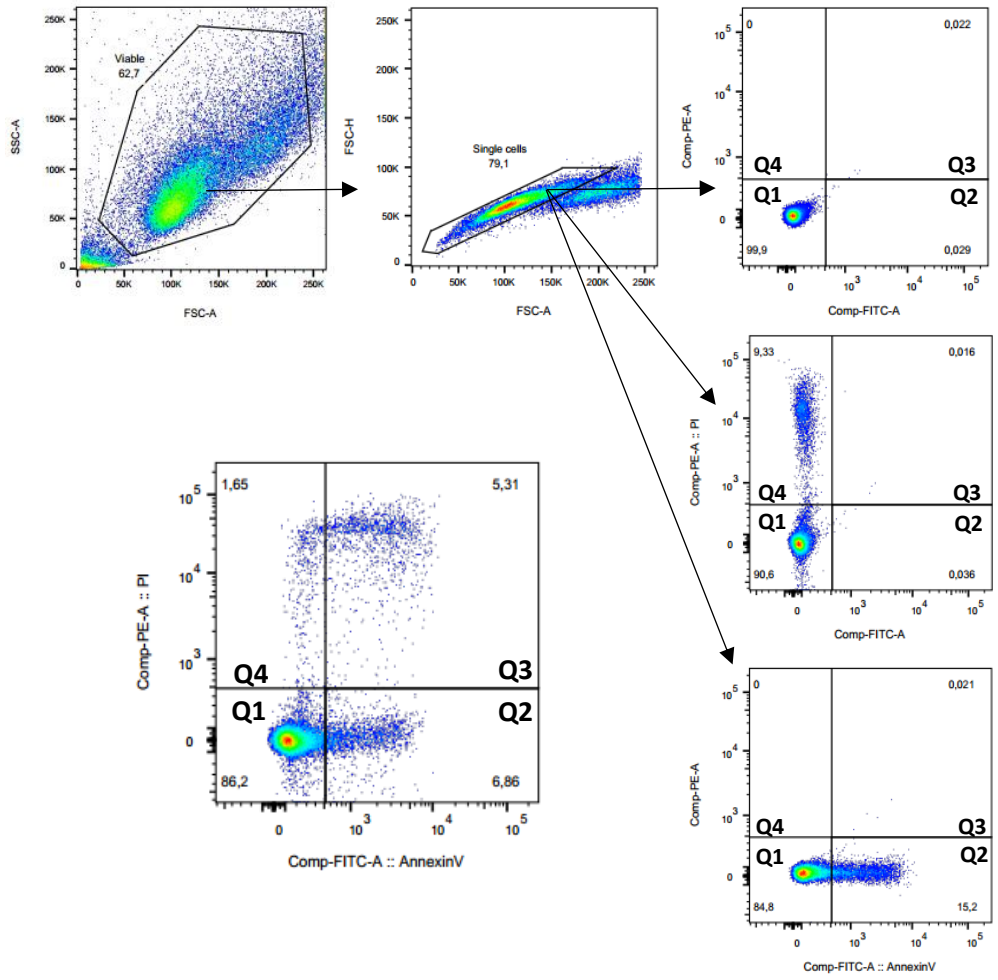

Figure 6. FACS gating strategy for apoptosis analysis in H1975 cells. Four quadrants were defined using the unstained control and the monolabels with annexin V or PI. The Q1 refers to PI^- ANX V^- cells (alive cells), Q2 PI^- ANX V^+(early apoptotic cells), Q3 PI^+ ANX V^+ (late apoptotic cells) and Q4 represents PI^+ ANX V^- (necrotic cells); Comp – compensation.

3.3.3. *IN VITRO* "LIQUID BIOPSY"

To assess the effect of docetaxel treatment in ctDNA release *in vitro*, cells culture medium was collected (liquid biopsy) and analysed. Briefly, 700000 H1975 cells were seeded in T25 flasks [VWR, Radnor, PA, USA] and incubated at 37ºC/5%CO_2. Cells were allowed to adhere and once 60%-80% confluence was reached cells were treated with different concentrations of docetaxel for 12h, 24h, 36h and 48h. After each time point, culture medium was collected and centrifuged at maximum speed (3180 g, 5 min) to remove cellular debris, and the supernatant stored at 4ºC until further use. Three independent experiments were performed.

3.3.4. DNA EXTRACTION AND CHARACTERIZATION

In order to reduce the initial volume for DNA extraction, culture medium samples were first concentrated using Amicon Ultra-15 mL Centrifugal Filters [Merck, Darmstadt, Germany], a filter system which allow the concentration of biological samples containing double-stranded DNA ranging from 137 to 1159 base pairs, with a concentration factor of 25x to 30x. Shortly, cell culture medium was placed in an Amicon filter system and centrifuged at maximum speed (3180 g) for 70min. The concentrate was collected to a new tube and stored at 4ºC until DNA extraction.

cfDNA was extracted using MagMAX Cell-Free DNA Isolation kit [Applied Biosystems, Life technologies, Waltham, MA, USA], a cfDNA extraction protocol based on magnetic beads. Briefly, binding/lysis buffer and dynabeads were added to each sample according to starting volume, and incubated for 10min with shaking to allow DNA binding to magnetic beads. After binding, beads were pelleted using a magnetic stand and the supernatant discarded. A sequence of washing steps were performed using a washing buffer and 80% ethanol to remove impurities. DNA was first eluted by Tris-acetate-EDTA (TAE) 0.1x solution [TE pH 8 + 10mM Tris-HCl + 1 mM EDTA]. Dynabeads and binding/lysis buffer were added again to DNA for a second cycle of extraction for sample purification. Three sequential washing steps with washing buffer and 80% ethanol were performed and DNA was finally eluted in 10 µL -20 µL of elution buffer. Eluted samples were stored at -20°C until further use.

DNA concentration was determined using Qubit® 2.0 Fluorometer [Invitrogen, Life technologies, Waltham, MA, USA], double stranded DNA high sensitivity (HS) assay. This assay utilizes a fluorescent dye specific for the target molecules, in this case DNA, and emit only when bound to target molecules allowing an accurate quantification. For *in vitro* liquid biopsy experiments, the quantification of DNA released in vehicle condition was subtracted to treatment conditions at each time point to exclude the basal levels of DNA release from the analysis. Additionally, all plasma samples' quantifications were normalized for volume of plasma collected in order to exclude differences derived from the initial amount of sample [cfDNA concentration(ng/mL of plasma) = cfDNA qubit quantification (ng/µL) x elution volume (µL) / plasma volume (mL)].

Fragment distribution and integrity of cfDNA was evaluated using 2200 TapeStation [Agilent Technologies, Santa Clara, CA, USA], an automated platform for capillary electrophoresis. This system is based on a fluorescent DNA intercalating agent that binds DNA and which intensity

allow the detection and quantification of the bands distributed in each electrophoresis capillary. High sensitivity DNA system [Invitrogen, Life technologies, Waltham, MA, USA] is designed for analyzing DNA molecules from 35 – 1000 bp and Genomic DNA Screen Tape [Invitrogen, Life technologies, Waltham, MA, USA] is designed for analyzing genomic DNA samples with a size ranging from 200 bp up to > 60000 bp. Both assays were applied to DNA samples. Briefly, all reagents were allowed to stabilize at room temperature. DNA sample buffer and the DNA sample were mixed in the defined proportion for each assay. The samples were vortexed for 1min and spin down. Finally, samples were placed in the Tape Station instrument. The results were analyzed with the TapeStation Analysis Software [Invitrogen, Life technologies, Waltham, MA, USA].

3.1.1. Real Time PCR

DIGITAL PCR

The mutational load of the T790M mutation in the formalin-fixed paraffin embedded (FFPE) H1975 cells-derived tumors was assessed by quantitative QuantStudio™ 3D digital PCR [Applied Biosystems]. This strategy uses TaqMan chemistry with dye-labeled probes to detect sequence-specific targets of mutated and wild-type (WT) DNA allowing absolute quantification and rare allele detection. The use of nanofluidic chips provides a tool to run thousands of PCR reactions in parallel of single molecules.

Briefly, to prepare the reaction mix 8.7 µL of master mix, 0.87 µL of TaqMan assay (primer/probe mix), 1.83 µL of H_2O and 6 µL of DNA sample (input 3 ng) was added in each reaction tube to a final volume of 15 µL. After mix preparation, dPCR reactions were loaded onto a QuantStudio™ 3D Digital PCR chip using the QuantStudio™ 3D Digital PCR chip loader. The following PCR conditions were used: 96°C for 10 min, 40 cycles at 62°C for 2 min and 98°C for 30 sec. After amplification chips were read using the QuantStudio™ 3D digital PCR instrument. Results were analyzed using the QuantStudio™ 3D AnalysisSuite™ Software. Representative image of data analysis is presented in Appendix 2.

INTPLEX® EGFR L858R/T790M KIT

The fraction of ctDNA present in the plasma of xenografted mice was quantified by real time quantitative PCR using the IntPlex® EGFR L858R/T790M kit [Dia Dx, Montpellier, France; kindly provided by Dr. Alain Thierry]. This kit include two primer sets: (1) T790M for specific detection

of T790M point mutation and (2) T790M WT primer set which amplifies a wild-type region of EGFR exon 20, near the mutation locus, allowing the quantification of total cfDNA. The quantification assays were performed in 96 well plates [TPP®, Trasadingen, Switzerland] in the CFX96 Touch™ Real-Time PCR Detection System [Bio-Rad Laboratories, Hercules, CA, USA], accordingly to recommended protocol.

Briefly, 12.5 µL of SYBR green mix, 7.5 µL of required primer sets and 5 µL of DNA sample (concentration between 3 and 1000 ng/mL of plasma) were added to each reaction well. PCR conditions were used accordingly to the manufacturer instructions: 95°C for 3 min, 40 cycles at 95°C for 5 sec and 30°C for 30 sec. DNA samples were run in triplicates for T790M primer set and duplicates for T790M WT set. Standards provided with the kit were used on each plate allowing the construction of a standard curve for relative quantification and PCR efficiency assessment. Non template control (NTC), a positive and negative sample for T790M primer set were used as controls (also provided with the kit).

The results were analyzed using the CFX manager® Software [Bio-Rad Laboratories, Hercules, CA, USA]. The mean quantity of ctDNA for each primer set was normalized to ng/mL of plasma per sample [cfDNA quantification (ng/mL of plasma) = cfDNA mean quantity (ng/µL) x elution volume (µL) / plasma volume (mL)]. Furthermore, the mutational load of samples positive for the T790M primer set was calculated as a percentage of cfDNA fragments carrying the mutation on all cfDNA fragments quantified [mutational load = T790M mutant circulating DNA concentration (ng/mL of plasma) x 100 / total circulating DNA concentration (ng/mL of plasma)].

3.1.2. IMMUNOHISTOCHEMISTRY

In order to prepare samples for histological analysis, each portion of the tumor was placed in a cassette and immersed in 10% formalin [Bio-optica, Milan, Italy] for 24h. After this period, cassettes were inserted in a tissue processor, where tissues were immersed in solutions of: 70% ethanol, 80% ethanol, 90% ethanol, 2x in 100% ethanol, 3x in Clear Rite for 1h each and in 2x Paraffin for 1h and 20 min each. Finally, tissues were embedded in paraffin wax for later analysis of histological sections. Tissue sections from all animals were obtained in coated slides [Thermo Scientific, Waltham, MA, USA], 3 µm each section, using the MICROM HM 335E microtome followed by incubation at 65ºC for 1 hour to adhere the sections to the slides. The sections were stored at room temperature (RT) until analysis.

To assess the correlation between the levels of cfDNA and apoptosis in the tissue upon docetaxel treatment, immunohistochemistry of tumor tissue sections was performed using the monoclonal antibodies mouse anti human anti-annexin V [Abnova, Taipei, Taiwan] and anti-KI-67 [Dako, Glostrup, Denmark], to measure apoptosis and proliferation, respectively. The target antigens were detected by chromogenic detection of the antibodies based on the activity of the horseradish peroxidase (HRP), an enzyme that forms a colored and insoluble precipitate upon addition of 3, 3 –diaminobenzidine substrate (DAB) substrate. For this purpose, samples were dewaxed with xylene [VWR, Radnor, PA, USA] (10 min in xylene and another 5 min in a new solution of xylene) and subsequently hydrated with ethanol (5 min in 100% ethanol, 5 min in 100% ethanol and 5 min in 70% ethanol) and with running water (5 min). For antigen unmasking, a citrate solution was prepared (citrate [Vector Labs, Burlingame, CA, USA] and H_2O type II, 1:100) in which the sections were immersed and incubated in a steam machine for 40 min. Samples were allowed to return to RT for 20 min. Tissues were washed twice with 0.1% PBS-T, for 5min, and then placed in a humid chamber with 1 mL of H_2O_2 solution (H_2O_2 [Sigma-Aldrich®, St. Louis, MO, USA] and methanol [VWR, Radnor, PA, USA], dilution 1:10), for 15 min, to block endogenous activity of peroxidases and prevent background signal. Next, the samples were washed using 0.1% PBS-T. For the blocking step, almost all liquid in the slides was removed and the tissues delimitated using a hydrophobic pen [Vector Labs, Burlingame, CA, USA]. Sections were then placed in the humid chamber with UltraVision Protein Block solution [Thermo Scientific, Waltham, MA, USA], enough to cover the tissue section, for 30 min at RT. Each section was probed overnight (ON) at 4ºC with an optimized concentration of the mouse anti-human annexin V (1:1500) or KI-67 (1:300) monoclonal antibodies diluted in antibody diluent [Thermo Scientific, Waltham, MA, USA], 100 µL per section. Since the detection method for each antibody was the same each section was probed with only one antibody. The next day, slides were washed 2x with 0.1% PBS-T to remove the primary antibody and, then, REAL EnVision detection system kit [Dako, Glostrup, Denmark] was used for signal detection. The kit includes a universal secondary antibody which was added to the tissue for an incubation of 30 min at RT, in the humid chamber. After washing the slides again, 100 µL of DAB, also included in the detection kit, was added to the slides in the humid chamber for 1min at RT, and immediately removed to avoid unspecific staining, with running water for 5 min. Finally, samples were stained with hematoxylin [Merck, Darmstadt, Germany] for 5 min, to mark the cells in the tissue, followed by 15 min in running water. Tissue was then dehydrated with ethanol (3 min in 70% ethanol, 5 min in 100% ethanol and 5 min in 100% ethanol) and dewaxed with xylene (5 plus 5 min). Samples were mounted using DPX mounting medium [Sigma-Aldrich®, St. Louis, MO, USA]

between the slide (25 x 75 x 1.0 mm) [Thermo Scientific, Waltham, MA, USA] and the coverslip (24 x 50 x 0.15 mm) [Normax, Marinha Grande, Portugal] and slides were analyzed under the optical microscope. Two to three complete and non-overlapping regions of interest (ROI) were selected for KI-67 and annexin V quantification analysis, and images were captured from a digital microimaging device, Leica DMD108 [Leica, Wetzlar, Germany], with a magnification factor of x200 times. For KI-67, a minimum of 500 neoplastic cells were analyzed and only nuclear staining was considered positive staining. Membrane or membrane plus cytoplasmic staining in neoplastic cells were considered positive for ANX V quantification. Focal membrane staining was also quantified as positive in tissue sections. Necrotic/highly apoptotic areas were excluded from the analysis due to loss of cell structure.

For histological analysis sections were stained with Hematoxylin and Eosin (H&E). For that, samples were dewaxed in xylene and alcohol as aforementioned. Next, samples were stained with Hematoxylin for 5 min and rinsed with running water, following by staining with alcoholic eosin [Thermo Scientific, Waltham, MA, USA] for 20 sec and then rinsed in water again (quick passage). The last processes were dehydration of the tissue sections with ethanol and diaphanization with xylene.

3.1.3. XENOGRAFT STUDIES

Subcutaneous xenograft models were stablished using human lung adenocarcinoma cells. H1975 human lung adenocarcinoma cells (1×10^5) re-suspended in 100 µL NaCl 0.9% were injected subcutaneously into the dorsal flank of 8-week-old to 14-week-old *Rag2*$^{-/-}$ *IL2rg*$^{-/-}$ immunodeficient C57BL/6 mice. Tumor growth was assessed every two days after detection of a small nodule. The tumor was measured with a digital caliper and volume calculated using the formula ($a \times b^2$) x 0.5 wherein *a* and *b* are the largest and the smallest diameters, respectively. When tumor size reached ~1200-1600 mm^3, mice were randomized into six groups (n = 6 to 7 per group) with equal representation of genders between experimental groups (Figure 7). One xenograft group (X) was used as control to establish the basal levels of DNA release into circulation of the tumor-bearing mice (0 mg/Kg of docetaxel treatment). Four xenograft groups (X) received a single dose treatment of docetaxel at two specific concentrations (10 mg/Kg and 25 mg/Kg), followed by euthanasia at two specific time points: 24h and 48h. Blood from non-xenografted mice (NX), were also collected from a non-treated group (0 mg/Kg of docetaxel treatment) and a treated group in the conditions described for xenograft mice. The treatment

was performed by intraperitoneal injection in the lower right quadrant of the abdomen with a 26 G needle, to a maximum volume of 500 µL. These experiments were performed with control condition (no treatment) and the effect of vehicle (treatment with drugs' diluent; n=3) in animals was also assessed.

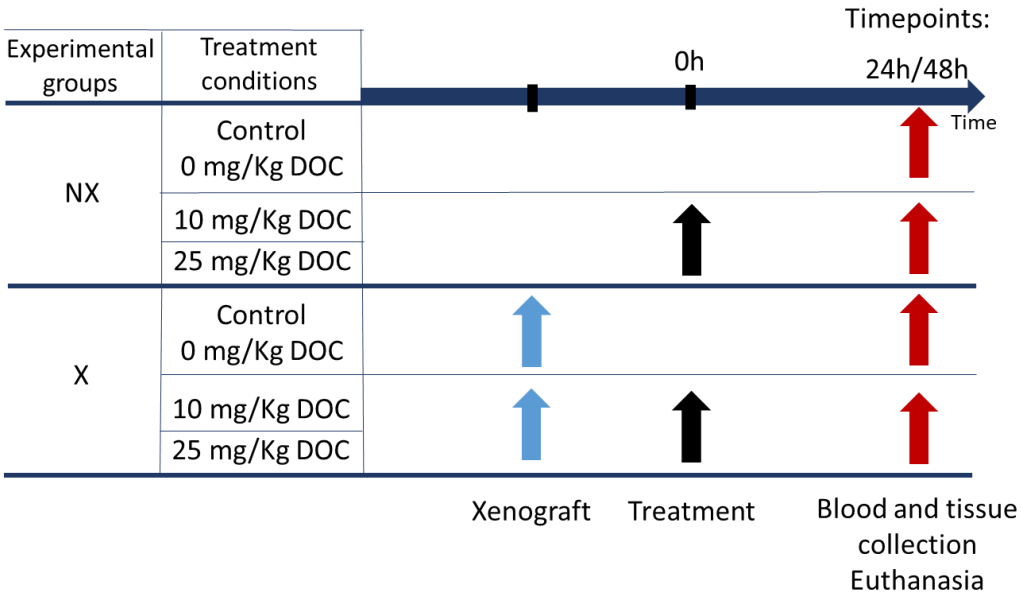

Figure 7. Experimental design of the *in vivo* studies. The diagram includes the cross-sectional analysis of blood and tumor tissue of non-xenografted (NX) and xenografted (X) mice submitted to different treatment conditions of docetaxel (DOC).

Physical appearance of the animals was observed every other day and their weight variations were monitored weekly, until sacrifice. Animals were anaesthetized with a volatile anesthetic (5% isoflurane, 1L/min oxygen) and the blood was collected by cardiac puncture into BD Vacutainer® blood collection tubes [BD Biosciences, San Jose, CA, USA], which were centrifuged (1200 g, 10 min) for separation of plasma from the blood cells compartment and frozen at -20°C. Up to 1000 µL of blood was collected from each mouse. After blood collection mice death was performed by cervical dislocation.

After sacrifice, mice tumors were rinsed in NaCl 0.9% (to remove fur) and cut in two equal parts. One portion was collected for cryopreservation (cryo vials were placed in a container with liquid nitrogen and then stored at -80°C), another for histological analysis (placed in a cassette and immersed in 10% formalin). Biological material collected from the animals are summarized in Appendix 1.

3.2. STATISTICAL ANALYSIS

For MTT assay IC50 was calculated and considered for analysis. The remaining experiments were evaluated using the Kruskall-Wallis (KW) test, a non-parametric test of one-way analysis of variance, for non-repeated measures, followed by a multiple comparison Dunnet's test, to compare all experimental groups with the control condition and groups with each other. For multiple comparisons two-way ANOVA was performed followed by Bonferroni's multiple comparison test to compare experimental groups. All tests were two-sided and the *P*-values were considered significant when inferior to 0.05. Statistical analysis was performed using the GraphPad Prism 6, for windows and all graphics were built using the same software. All graphics represent the mean values ± standard deviation (SD).

4. RESULTS

4.1. EFFECT OF DRUG TREATMENT ON LUNG CANCER CELL LINES

4.1.1. CELL VIABILITY

In order to assess the effect of widely used chemotherapeutic drugs in the viability of lung cancer cell lines indirectly by their enzymatic activity, MTT assay was performed (Figure 8 (A)). Since no significant differences were observed between the untreated and vehicle treated conditions the results are presented with the vehicle condition as control. Docetaxel treatment in H1975 and A549 cells induced a concentration and time-dependent reduction on viability of cells. As illustrated in Figure 8 (A) the viability of cells, following 0.01 μM docetaxel exposure, was reduced from 80% to 60% and 40% of viable cells at 24h, 48h and 72h, respectively. Additionally, 0.01 μM docetaxel treatment caused a time-dependent reduction in viability of A459 cells, whereas no differences were observed on H1975 cells. Surprisingly, higher concentrations of docetaxel (1; 10 μM) induced, on both H1975 and A549 cells, an increase in the percentage of viable cells along time when compared to 0.1 μM concentration. As illustrated in Figure 8 (B) the IC50 values at 72h for the cell lines exposed to docetaxel treatment were 0.03 μM for H1975 cells and 0.02 μM for A549 cells.

As to gemcitabine, no effect was observed on the viability of cells 24h after treatment at any concentration neither for H1975 or A549 cells. However, a reduction on viability of H1975 cells was observed for prolonged exposure to 0.01 μM (80% and 70% of viable cells at 48h and 72h, respectively), an effect more evident for higher concentrations of gemcitabine. A similar behavior was observed for A549 cells exposed to 0.01 μM of gemcitabine, at 48h and 72h time point. The reduction in viability of A549 cells was more pronounced for 0.1 μM gemcitabine even though, higher concentrations have shown a similar effect to the one observed for 0.1 μM. The IC50 values at 72h for the cell lines exposed to gemcitabine treatment were 0.653 μM and 0.241 μM for H1975 and A549 cells, respectively (figure 8 (B)).

Regarding carboplatin, an effective reduction on the viability of cells was only observed for prolonged exposure (48h and 72h) of H1975 cells to high concentration (10 and 100 μM). As to A549 cells the effect of carboplatin was more pronounced for 100 μM concentration, at 48h and 72h time points. Since the effects of carboplatin were only observed at higher concentrations, the IC50 values were 50.99 μM for H1975 cells and 265.80 μM for A549 cells (figure 8 (B)). No effects on the viability of HCC827 cells were observed for the drugs concentrations tested.

A

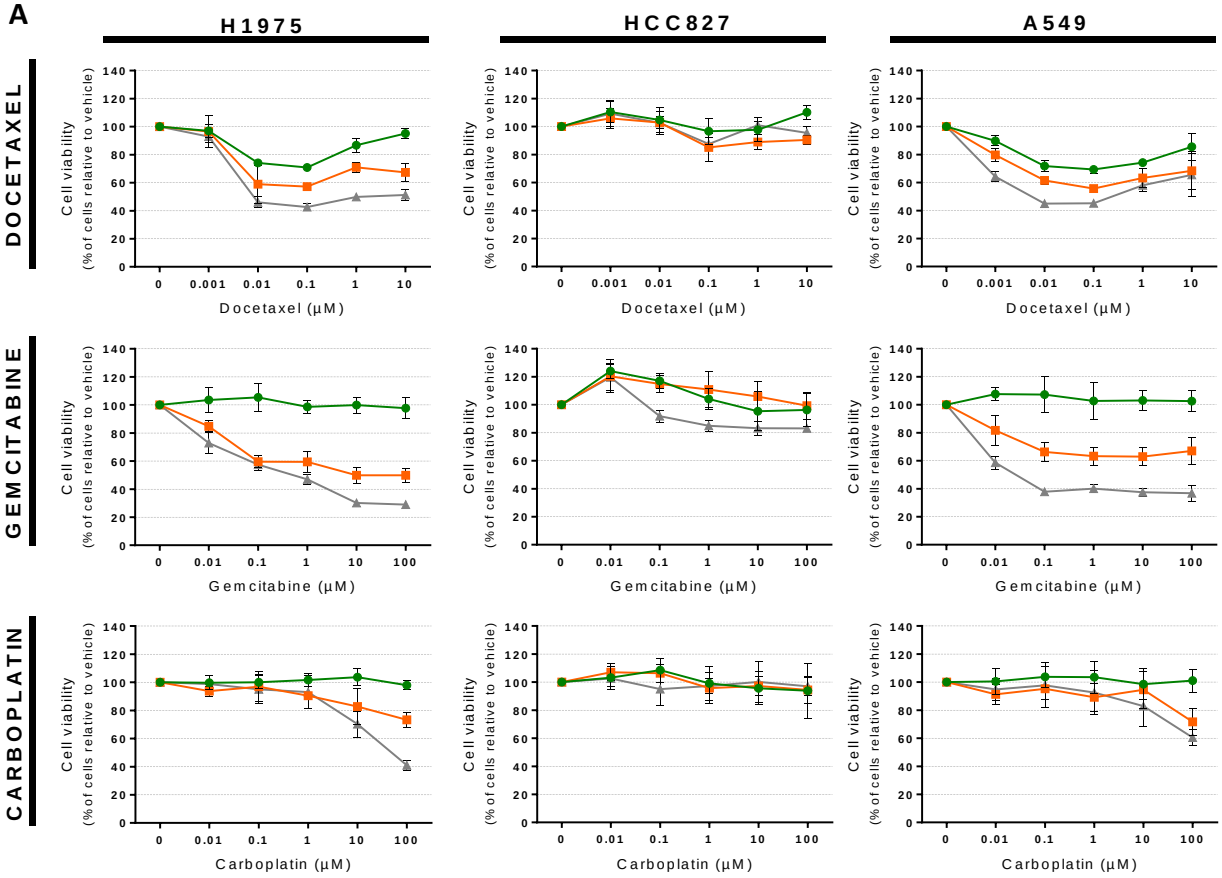

B

IC50 (µM)	H1975	A549	HCC827
Docetaxel	0.03 [0.02 to 0.05]	0,02 [0.01 to 0.03]	>10000
Gemcitabine	0.653 [0.42 to 1.03]	0,24 [0.08 to 0.70]	>10000
Carboplatin	51.00 [35.65 to 72.96]	265,80 [85.82 to 823.40]	>10000

Figure 8. Quantification of cell viability by a MTT assay. [A] Viability of lung cancer cell lines (H1975, HCC827 and A549) upon treatment with increased concentrations of chemotherapeutic drugs (docetaxel, gemcitabine and carboplatin), for 24h (green), 48h (orange) and 72h (grey) as stated in Material and Methods section. The results are expressed as a percentage (%) normalized to vehicle condition, representing the mean ± SD of 3 independent experiments carried out with 6 replicates. [B] IC50 values of the drugs tested for different cell lines following 72h of exposure are presented on the table with 95% confidence interval (CI).

4.1.2. CELL APOPTOSIS

H1975 cells were treated with 0.001 µM and 0.1 µM docetaxel for 12h, 24h, 36h and 48h in order to assess the dose and time dependent effect of docetaxel on apoptosis levels (Figure 9). The drug concentrations and exposure times were selected accordingly to the results obtain for cells' viability (see section 4.1.1 results). Upon treatment with 0.1 µM of docetaxel, an increase in early apoptosis (Q2 - PI^- ANX V^+ cells) was observed at all time points when compared to vehicle condition (Figure 9 (B)). A major increase was observed 24h after treatment (Bonferroni's test, $P<0.0001$) with a subsequent decrease at 36h and 48h when compared to 24h time point (Bonferroni's test, $P<0.0001$) (Figure 9 (B)). Regarding late apoptosis (Q3 – PI^+ ANX V^+ cells), a significant increase was observed 36h and 48h following treatment with 0.1 µM of docetaxel when compared to the vehicle condition (Bonferroni's test, $P<0.0001$). The effect was greater at 48h as illustrated in Figure 9 (C). The treatment with 0.001 µM docetaxel had no effect on apoptosis levels (Bonferroni's test, $P>0.05$). Overall, a time-dependent reduction on viable cells (Q1 – PI^- ANX V^- cells) was observed for 0.1 µM docetaxel treatment (Bonferroni's test, $P<0.0001$). Necrosis (Q4 – PI^+ ANX V^- cells) was also significantly different from the vehicle condition at 24h, 36h and 48h time points for 0.1 µM docetaxel (Bonferroni's test, $P<0.001$, $P<0.001$ and $P<0.0001$, respectively) (Figure 9 (D);(E)).

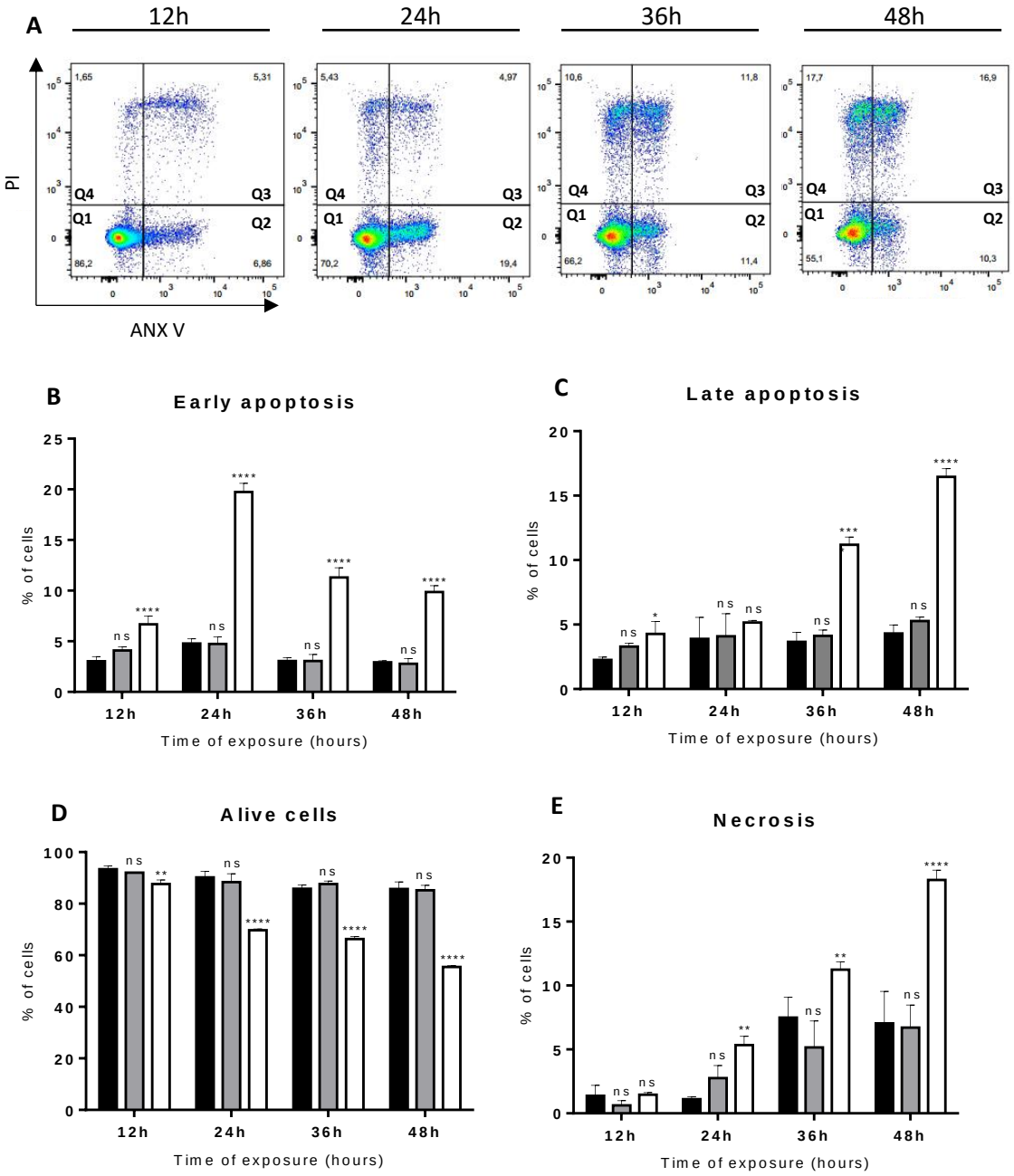

Figure 9. Effects of docetaxel on apoptosis of H1975 cells. (A) Scatter diagram of the flow cytometry of H1975 cells treated with 0.1 µM docetaxel for 12h, 24h, 36h and 48h according to the protocol in Material and Methods. Q1 - PI^- $ANX\ V^-$ cells (alive cells), Q2 - PI^- $ANX\ V^+$(early apoptotic cells), Q3 - PI^+ $ANX\ V^+$ (late apoptotic cells) and Q4 - PI^+ $ANX\ V^-$ death cells (necrotic cells). Percentage of early apoptotic cells (B), late apoptotic cells (C), alive cells (D) and necrotic cells (E) for the vehicle condition (black bars), and for cells exposed to 0.01 µM docetaxel (light grey bars) or to 0.1 µM docetaxel (white bars) at 12h, 24h, 36h and 48h time points. Data represent the mean ± SD of one independent experiment carried out in triplicate. Statistical analysis was performed by Bonferroni's test (2 way ANOVA). * represent statistically significant differences in apoptosis compared to vehicle condition: ns - *P*>0.05; * *P*<0.05 ** *P* <0.01; *** *P* <0.001; **** *P* <0.0001.

4.2. IMPACT OF DOCETAXEL TREATMENT ON DNA RELEASED FROM H1975 CELLS

The DNA extracted from the supernatant of H1975 cells treated with docetaxel was quantified to evaluate the impact of docetaxel treatment on DNA release levels (figure 10). As illustrated in Figure 10, there were no differences on DNA released from H1975 cells treated with 0.001 µM, at any time point (Bonferroni's test, *P*>0.05). However, upon treatment with the highest concentration (0.1 µM), an increase on DNA release levels were observed when compared to the lower concentration (0.001 µM) for all time points (Two-way ANOVA, *P*<0.01). Also, a significant increase on DNA levels was observed each 24h, i. e., 24h to 48h (Bonferroni's test, *P* <0.01) and also for 12h interval, 36h to 48h (Bonferroni's test, *P* <0.05). However, for the others 12h intervals, i. e., 12h and 24h, 24h and 36h and also a 24h interval, 12h and 36h no significant differences were observed (Bonferroni's test, *P* >0.05).

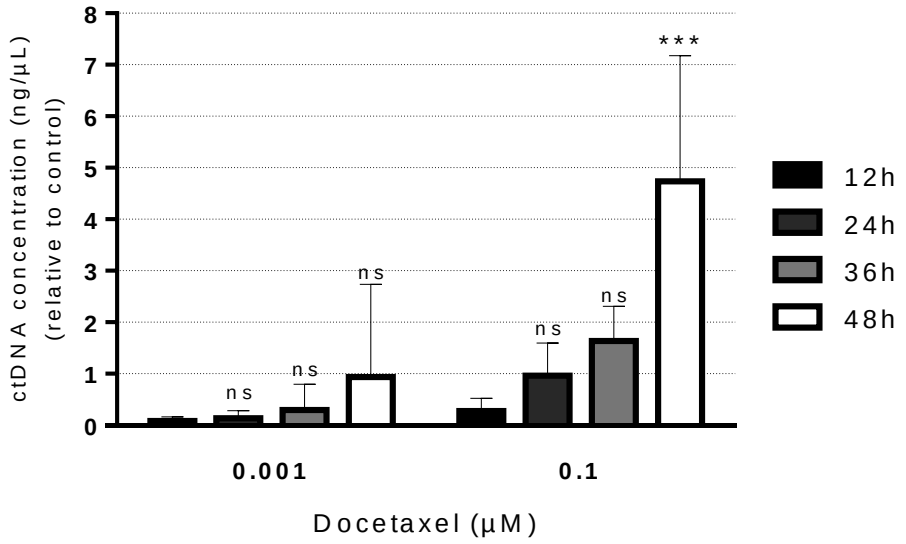

Figure 10. ***In vitro*** **liquid biopsy analysis**. DNA levels extracted from the supernatant of H1975 cells treated with 0.001 µM and 0.1 µM docetaxel as described in the Material and Methods. The results are expressed as concentration relative to vehicle condition, and represent the mean ± SD of three different experiments. * represent statistically significant differences between relative DNA levels released at 24h, 36h and 48h, comparing to DNA released at 12h: ns - *P*>0.05; *** *P* <0.001.

4.3. TUMOR GROWTH KINETICS IN XENOGRAFT MICE MODEL OF H1975 CELLS-DERIVED TUMORS

In vivo experiments were performed using a subcutaneous xenograft immunodeficient mice model (Figure 11 (B)). The tumors from mice xenografted with H1975 cells were highly vascularized and encapsulated as illustrated in Figure 11 (C);(D). The tumor growth, illustrated in figure 11 (A), was assessed since the appearance of a small nodule, approximately at day 24. Approximately one month after engraftment the tumors reached the volume stablished for treatment (1200-1600mm^3). From a total of 32 xenografted mice, 28% (9/32) developed ulceration in the surface of the tumor and exhibited delayed tumor growth rates.

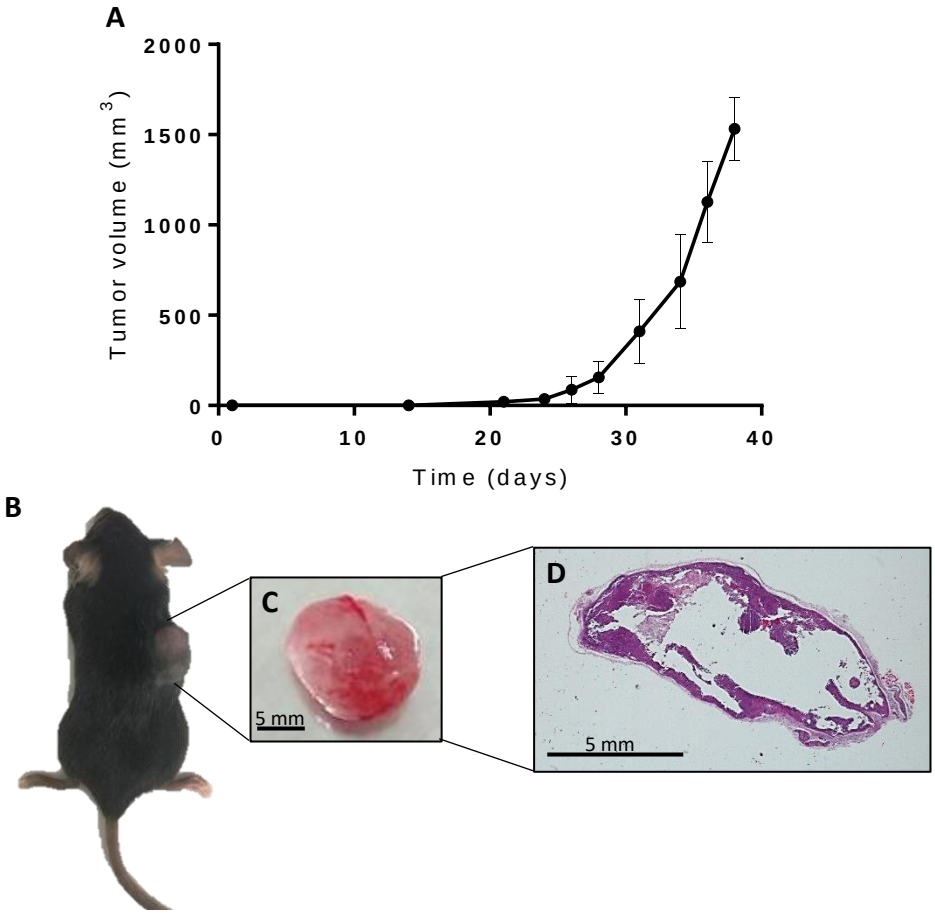

Figure 11. Tumor growth kinetics of H1975 cells-derived tumor in xenograft mice model. (A) representative curve of tumor growth kinetics (data randomly selected from 5 xenografted animals without ulceration); (B) subcutaneous localization of the H1975 cells xenograft; (C) representative tumor from H1975 cells after removal from the mice; (D) H&E of H1975 cells-derived tumor section representative of the encapsulated structure of the tumors.

4.4. EVALUATION OF DOCETAXEL TREATMENT ON TUMOR TISSUE PROLIFERATION AND APOPTOSIS

The effects of docetaxel treatment on tumors tissue' proliferation and apoptosis were assessed by IHC. Regarding proliferation, quantification of KI-67 nuclear staining for the groups treated with docetaxel for 24h revealed no significant differences when compared to the untreated xenografted mice (Dunn's test, $P>0.05$) (figure 12 (B);(D) and (F)). A slightly decrease in the proliferation of cells was observed in tumors collected 48h after treatment with 10 mg/Kg (Dunn's test, $P>0.05$) and 25 mg/Kg (Dunn's test, $P>0.05$) docetaxel (figure 12 (F)). Annexin V membrane staining was used to measure the levels of apoptosis in the tumor tissue (figure 12 (C)). As illustrated in Figure 12 (E);(G) apoptosis levels in the tumor tissue of mice treated for 24h with docetaxel showed no differences relative to the tumors of untreated mice (Dunn's test, $P>0.05$). However, tumors collected from mice treated for 48h with docetaxel revealed an increase in apoptosis levels which was significantly higher in mice treated with 25 mg/Kg docetaxel (Dunn's test, $P<0.01$) when compared to untreated xenografted mice (figure 12 (G)). As demonstrated in Figure 12 (G) the increase in apoptosis levels was dose and time-dependent since for the same concentration of docetaxel it increased with the time of exposure to treatment, with a greater impact for the higher concentration (Dunn's test, 10 mg/Kg docetaxel – $P>0.05$; 25 mg/Kg docetaxel – $P>0.05$). Necrotic or highly apoptotic areas were observed in 56% (18/32) of the cases.

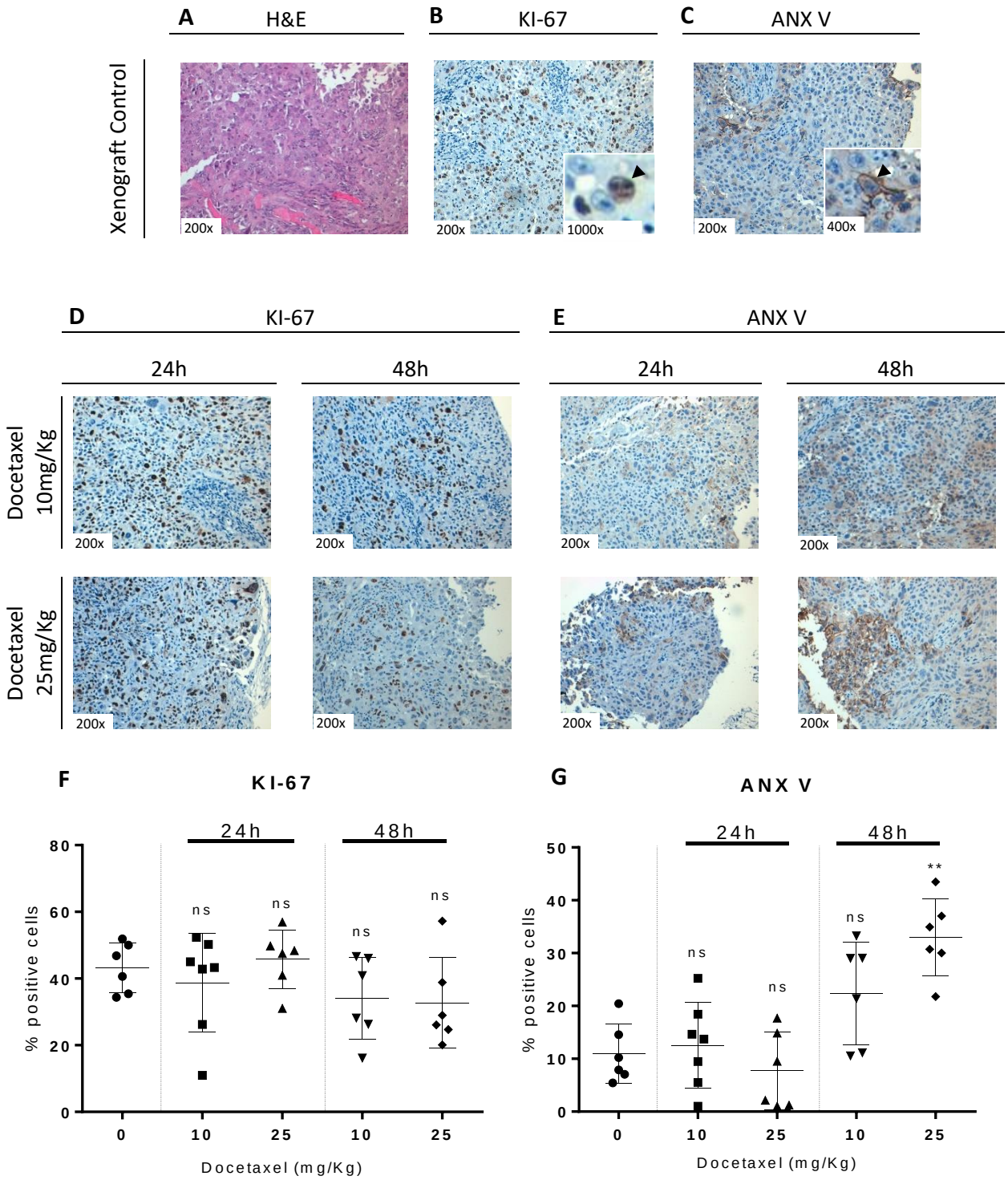

Figure 12. Tumor tissue proliferation and apoptosis. Representative images of control condition with (A) H&E staining; (B) ki-67 immunostaining (nuclear localization – arrow head); (C) annexin V immunostaining (membrane localization – arrow head). Representative images of tumor sections of mice treated with docetaxel (10mg/Kg or 25mg/Kg) for 24h or 48h are presented for KI-67 immunostaining (D) and annexin V immunostaining (E). The percentage of positive cells stained for KI-67 (F) or annexin V (G) were determined for the different treatment conditions and time points, as described in Material and Methods (n= 6 or 7). Horizontal line represent mean values ± SD. Statistical analysis was carried out by Dunn's test. * represent statistically significant differences for proliferation and apoptosis at 24h and 48h time points: ns - *P*>0.05; ** *P* <0.01.

The correlation between the rate of proliferation and apoptosis was assessed for the control condition and the groups treated with docetaxel 25 mg/Kg (Figure 13). It was possible to observe a negative correlation between the two variables r^2=0.2519 (Pearson correlation, *P*<0.05), which means that when one variable increases the other decreases. Overall, the results have shown the presence of one cluster including untreated animals (control condition) and treated for 24h (Figure 13, green circle). This cluster is characterized by higher proliferation rate and low levels of apoptosis. Another cluster was identified with lower proliferation rate and higher level of apoptosis which included exclusively animals treated with docetaxel for 48h (Figure 13, red circle).

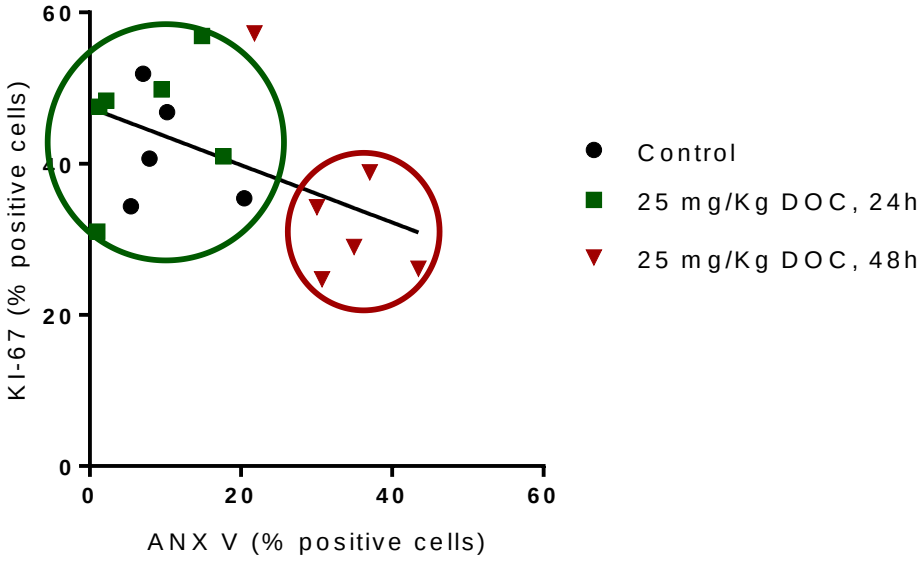

Figure 13. Correlation between proliferation and apoptosis rates in tumor tissue. Tissue from animals without treatment and treated with docetaxel 25 mg/Kg for 24h (green dots) or 48h (red dots) selected to determine the correlation between proliferation and apoptosis in the tissue. Green and red circles represent the two clusters identified. Each dot represents one animal. Correlation is represented through linear regression (black line). DOC: docetaxel.

4.5. EFFECT OF DOCETAXEL TREATMENT ON DNA RELEASE IN PLASMA FROM XENOGRAFT MICE

4.5.1. cfDNA FRAGMENTATION PROFILE

In order to characterize the cfDNA from the plasma of all animals the fragment size distribution was assessed based on fragmented DNA concentrations (Figure 14). Results revealed a highly fragmented pattern of cfDNA with a major representation of DNA with ≈183 bp (≈80% of total

cfDNA). Fragments of ≈375 bp and ≈579 bp were observed with decreased representation, ≈12% and 3%, respectively. The DNA longer than 700 bp comprises fragments up to 1316 bp.

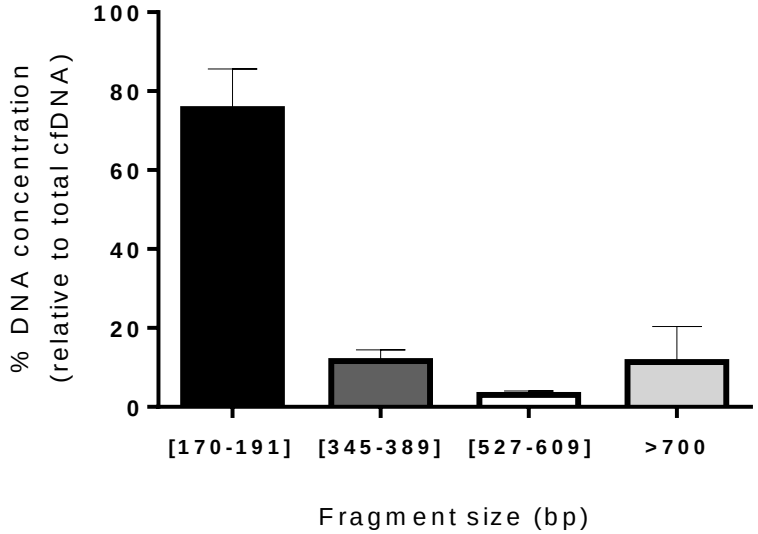

Figure 14. cfDNA fragmentation profile. Fragment size distribution presented as percentage of total cfDNA quantified (100%). Total and fragment quantifications were obtained using Tape Station System as described in Material and Methods.

4.5.2. CFDNA CONCENTRATION IN PLASMA

The results obtained *in vitro* regarding the levels of cfDNA suggested an impact of docetaxel treatment on DNA released from H1975 cells. Thus, the effects of docetaxel treatment on the cfDNA levels in the plasma of H1975 cells xenograft mice were assessed (figure 15). No differences were observed between untreated and vehicle treated conditions. Non-xenograft mice receiving no docetaxel treatment have shown an average total cfDNA of 4,1 ng/mL plasma. Administration of docetaxel induced no differences on total cfDNA release levels by non-xenografted mice independent of the duration of treatment (KW, $P>0.05$) (figure 15(A)). As to H1975 cells xenografted mice, the results have shown increased levels of total cfDNA in plasma of mice for any treatment condition tested. Mice treated with the highest concentration of docetaxel tested (25 mg/Kg) revealed increased levels of total cfDNA at 24h (Dunn's test, $P<0.05$) and 48h (Dunn's test, $P<0.05$) (figure 15(B)). However, for xenografted mice treated with 10 mg/Kg docetaxel no significant differences were observed in the total cfDNA release levels even for prolonged time of exposure (24h: Dunn's test, $p>0.05$; 48h: Dunn's test, $p>0.05$), when compared to the untreated mice (control condition). A dose dependent effect of docetaxel on the levels of total cfDNA was observed for mice treated with a high concentration of docetaxel (25mg/kg) when compared to the lower concentration (10 mg/Kg), at both time points.

Regarding the smaller fragment of cfDNA for each animal (≈183 bp) the results were rather similar to the ones obtained for total cfDNA. According to Figure 15 (C), no differences were observed on fragmented cfDNA release levels by non-xenografted mice independent of the duration of treatment (KW, *P*>0.05). As illustrated in Figure 15 (D), significant higher levels of fragmented DNA were released in the plasma of xenografted mice treated with 25 mg/Kg docetaxel (24h: Dunn's test, *P*<0.01; 48h: Dunn's test, *P*<0.05), with a dose and time dependent effect, opposing to what was observed for xenografted mice exposed to 10 mg/Kg docetaxel (Dunn's test, *P*>0.05).

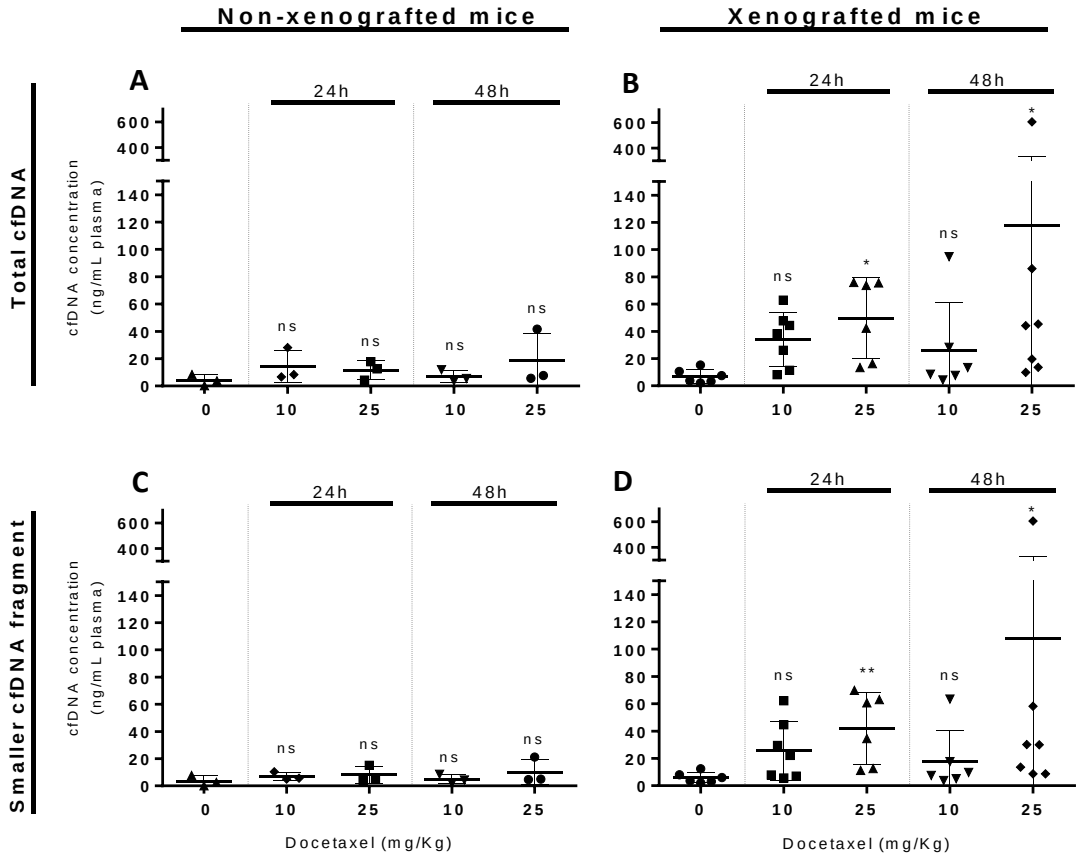

Figure 15. cfDNA concentration levels from plasma of mice models. Total cfDNA concentration in non-xenografted mice (A) and xenografted mice (B) in plasma collected 24h and 48h after treatment with Docetaxel (10 or 25mg/Kg). Quantification of the smaller fragment of DNA extracted from non-xenografted mice (C) and xenografted mice (D) at the same time points. Horizontal line represents mean ± SD of a total of at least 3 animals for non-xenografted group, and 6 to 7 animals for xenografted group. * represent statistically significant differences between cfDNA levels for the two drug concentrations at 24h and 48h, comparing to untreated condition for non-xenografted and xenografted conditions: ns - *P*>0.05; * *P*<0.05; ** *P*<0.01.

4.5.3. CTDNA FRACTION IN TOTAL CFDNA AND MUTATIONAL LOAD

The reference mutational load of the DNA from H1975 cells-derived tumors was determined using digital PCR and corresponded to 82% (% of mutated DNA sequences in total DNA quantified). In order to clarify the presence and amount of ctDNA in the total cfDNA quantified in plasma samples a real time quantitative PCR was performed (see Appendix 3). This assay uses human-specific primer sets which allow exclusively quantification of total (EGFR fragments) or mutated (T790M positive) ctDNA derived from human H1975 cells-xenograft. In order to confirm the specificity of the human-specific primer sets, DNA extracted from mouse's spleen was analyzed and there was no DNA amplification. Overall, this preliminary analysis revealed that total ctDNA was increased following docetaxel treatment when compared to untreated xenografted mice (control condition) (Figure 16 (A)). Specifically, animals treated with docetaxel for 24h have shown a dose dependent increase in total EGFR ctDNA levels. The lowest mean levels of ctDNA were observed at 48h time point for the mice treated with 25 mg/Kg docetaxel whereas the mice treated with 10 mg/Kg docetaxel for this time point included the highest mean ctDNA quantification. Additionally, mutational load was calculated based on the fraction of mutated ctDNA in the total ctDNA quantified and revealed no mutated DNA quantification in the untreated xenograft mice (Figure 16 (B)). Regarding treated xenograft mice, it was possible to quantify mutated ctDNA in every treatment conditions without any differences between them.

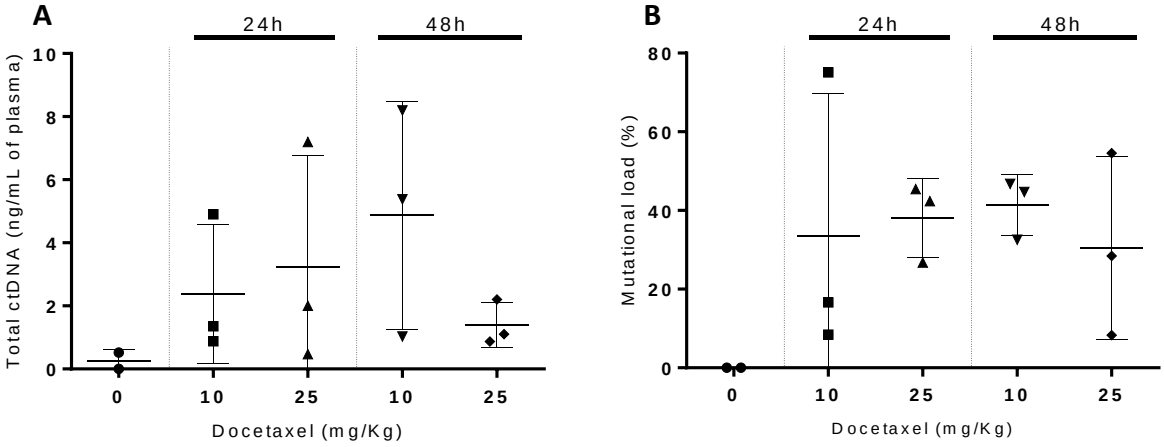

Figure 16. Total ctDNA quantification and mutational load calculation. Graphical representation of total ctDNA quantification (T790M WT positive) (A) and T790M mutational load (B). Horizontal lines represent mean ± SD; n=2 or 3.

5. DISCUSSION

The study of tumor-derived DNA, as a liquid biopsy strategy, may represent an alternative to the limiting standard tissue biopsy approaches, since it was discovered to mirror tumor genetics in the circulation of cancer patients (74,78). In fact, technological advances for detection and characterization of ctDNA have revealed its potential clinical relevance as a biomarker for management of cancer (71). Despite exciting breakthroughs, sensitivity of methodologies available for detection of quantifiable and high quality ctDNA are still below optimal levels for clinical application (75,95). Hence, new strategies are required to overcome these limitations which may rely on knowledge of the biology and dynamics of ctDNA. In this work, with the goal to increase ctDNA levels, cytotoxic chemotherapeutic drugs were used as a driver of apoptosis and, consequently, of DNA release from tumors into circulation.

Our first approach was to perform a drug screening in several lung cancer cell lines in order to assess the effect of treatment on the viability of cells. H1975 cells were used as they represent a relevant model of disease, harboring a specific resistant mutation to TKIs therapies with major clinical relevance (99). Upon treatment with gemcitabine no differences were observed on the viability of cells after 24h of exposure. This effect is probably caused by the arrest of cells in S phase, as an initial consequence of the mechanism of action of gemcitabine which inhibits DNA synthesis culminating in cell apoptosis at later time points, as already demonstrated for pancreatic cancer cell lines (100). Regarding carboplatin, it was only effective at reducing the viability of cells at high concentration. However, this results do not respond to the objectives of our study which intends to assess a minimal effective drug to induce loss of cells viability, in order to avoid drug toxicity problems. The results obtained revealed that, overall, docetaxel was the drug with greater impact on the viability of H1975 cells at lower concentrations in spite of the slightly increase on the viability of cells observed for higher drug concentration. The mechanism by which docetaxel induced apoptosis upon interaction with the microtubules is not fully understand (101). Nevertheless, it has been proposed that lower and higher concentrations of taxanes induce cell cycle arrest and apoptosis through different mechanisms which might explain the double effect observed (102). Docetaxel is a cytotoxic drug with expected impact on cell apoptosis which prompted the study of its effects on cell apoptosis (103). Therefore, cytometry experiment for apoptotic markers were performed, allowing the identification of different stages of apoptosis to assess the time-dependent effect of the drug. The results have shown that cells treated with docetaxel at 0.1 µM entered early stages of apoptosis mainly 24h

after treatment. The reduction observed in viable cells at 24h (see section 4.1.1 results) might be due to cell cycle arrest at G2-M phases and only about 24h after docetaxel treatment it activates apoptotic mechanisms in H1975 cells. Activation of apoptotic process by docetaxel treatment was confirmed by increased levels of late stage of apoptosis in H1975 cells observed for prolonged time of exposure. This data correlates with a greater reduction in viable cells observed at later time points. The presence of DNA in the supernatant of H1975 cells following docetaxel treatment was assessed since the apoptotic process was associated with DNA release levels (61). Accordingly, a significant increase was observed in the levels of DNA released from H1975 cells exposed to 0.1 µM docetaxel for 48h. In addition, the profile of DNA release levels over time was closely related to the profile of late apoptosis rate induced by docetaxel treatment, indicating a strong impact of docetaxel treatment in DNA release mediated by apoptosis.

In order to optimize the methodology for ctDNA as liquid biopsy in a more complex biological setting mimicking closely the tumor context a pilot study was performed *in vivo*. Similarly to *in vitro* studies, two concentrations of docetaxel were selected taking in consideration drug pharmacokinetics and dose conversion between mice and human (104,105). Importantly, the tumor volume selected to treatment was near the humane endpoint (2000 mm^3) to mimic advances stages of lung cancer, the most common diagnosed stages of disease and the one with increased levels of cfDNA observed in xenograft mice models (106). Similarly to what was performed *in vitro*, the first approach *in vivo* consisted on the evaluation of docetaxel treatment effects on tumor tissue apoptosis. Interestingly, the results revealed a slightly decrease on proliferation of tumor cells which correlated with an increase in apoptosis levels for the higher concentration and prolonged exposure, i.e. 24h to 48h. Additionally, apoptotic cells were mainly localized near blood vessels and in the borders of the tumor. These results might be explained by the limit distribution and penetration of docetaxel into tumor cells as a result of the tumor vascularization and the tumor microenvironment, composed of cells besides tumor cells. A study has already described that, in solid tumors, the limit distribution of taxanes works as a mechanism of resistance (107). Although uncertain, the presence of highly apoptotic or necrotic areas observed in the tissue might indicate an earlier effect of docetaxel in the tissue. Accordingly to the literature, high fragmentation pattern of the cfDNA is related to DNA from apoptotic origin (61). Indeed, in the present work it was observed high proportion of smaller DNA fragments in the cfDNA collected from mice exposed to docetaxel. This data correlates with the increased levels of apoptosis observed in the tumor tissue. Additionally, the presence of

bigger fragments observed in the plasma samples might indicate other mechanisms of DNA release triggered by docetaxel treatment, such as necrosis (61).

Regarding the levels of total cfDNA in the plasma of mice, animals without tumor did not show an increase in the levels of total cfDNA after docetaxel treatment (25mg/Kg) when compared to xenografted mice in the same conditions. Therefore, the results indirectly suggest the tumor as the major source of DNA detected in circulation rather than normal cells which may be in part justified by a certain degree of specificity of chemotherapeutic drugs for highly proliferative cells. Moreover, increased levels of cfDNA following prolonged time of exposure (48h) might be the consequence of the increased levels of apoptosis observed in the tumor tissue at this time point. However, the increased levels of cfDNA 24h after docetaxel treatment do not correlate with the apoptotic rates observed in the tissue at this time point suggesting other mechanism of cfDNA release, such as active release of microvesicles. In fact, it has been demonstrated that cells under stress conditions such as drug treatment might alter the extent of active microvesicles secretion, namely exosomes (108).

Docetaxel targets highly proliferative cells; however it is not specific for tumor cells which rise the question whether the DNA detected in circulation is in fact derived from the tumor. Although the previous results suggest the tumor as the origin of cfDNA, a human specific primer for EGFR was used to quantify specifically tumor DNA. Although preliminary and despite the high variability within groups, it was possible to detect increased levels of total ctDNA in circulation after a single treatment with docetaxel. The variability is clearly demonstrated by a sample treated with 25 mg/Kg docetaxel at 48h time point (section 4.5.3 results) that have shown high levels of total ctDNA and it was almost negative for mutated ctDNA which justify the need of further studies to clarify these results. The mutational load of xenografted mice treated with docetaxel was below the % of mutated ctDNA expected from the reference mutational load of the tumor tissue (82%). Nevertheless, the results indicate an increased sensitivity of detection of low abundant mutated DNA derived from the tumor upon treatment with docetaxel when compared to the control condition. Altogether, this data demonstrate the impact of docetaxel treatment on tumor cells which culminated in increased levels of total and mutated ctDNA.

.

6. CONCLUSIONS AND FUTURE PERSPECTIVES

This pilot study gave new insights into a new possible strategy to overcome the low sensitivity of detection of ctDNA. Despite preliminary, we have shown higher levels of cfDNA *in vivo* upon treatment with a single dose of docetaxel at 25 mg/Kg for 48h. Analysis of the tissue revealed increased levels of apoptosis at the same treatment conditions. Moreover, the characterization of the fragmentation profile of the cfDNA corroborate the hypothesis that the ctDNA was derived from apoptotic processes, which indicates the impact of docetaxel treatment in cells' apoptosis and consequently ctDNA levels in circulation.

The results obtained in this pilot study might be used to design a more robust and representative *in vivo* experiment in order to corroborate the present findings. Additionally, the use of a transgenic mouse model which spontaneously develop lung cancer now available in the lab will also represent a valuable tool to mimic more accurately the process of tumorigenesis, namely in terms of tumor irrigation and angiogenesis which are crucial for this study.

These results are preliminary and further studies are required to support the conclusions. Thus, we plan to expand this study to the A549 cell line and gemcitabine treatment which have shown promising results *in vitro*.

Furthermore, evaluation of other mechanisms of origin of ctDNA, such as active release of ctDNA, or necrotic processes, might help to clarify some of the results obtained for ctDNA/cfDNA quantifications.

Finally, it would be of interest to expand this study to different cancer models since the principles of tumor cell proliferation and ctDNA release in which this study relies are common to all types of cancers. Different categories of drugs might also be considered, such as immunomodulatory drugs, to optimize the impact of treatment on ctDNA release.

7. REFERENCES

1. Du W, Elemento O. Cancer systems biology: embracing complexity to develop better anticancer therapeutic strategies. Oncogene. 2014;34:3215–25.

2. Suvà ML, Riggi N, Bernstein BE. Epigenetic reprogramming in cancer. Science. 2013;339(6127).

3. Tomasetti C, Vogelstein B, Cancer SK, Hopkins J, Cancer K. Variation in cancer risk among tissues can be explained by the number of stem cell divisions. Science. 2016;347(6217):78–81.

4. Stratton MR. Exploring the Genomes of Cancer Cells: Progress and Promise. Science. 2011;331(6024):1553–8.

5. Evan GI, Vousden KH. Proliferation, cell cycle and apoptosis in cancer. Nature. 2001;411(6835):342–8.

6. Vogelstein B, Papadopoulos N, Velculescu VE, Zhou S, Diaz LA, Kinzler KW. Cancer genome landscapes. Science. 2013;339(6127):1546–58.

7. Robert J. Biology of cancer metastasis. Bulletin du Cancer. 2013;100(4):333–42.

8. Alizadeh AA, Aranda V, Bardelli A, Blanpain C, Bock C, Borowski C, et al. Toward understanding and exploiting tumor heterogeneity. Nat Med. Nature Publishing Group; 2015;21(8):846–53.

9. Marusyk A, Almendro V, Polyak K. Intra-tumour heterogeneity: a looking glass for cancer? Nat Rev Cancer. Nature Publishing Group; 2012;12(5):323–34.

10. Quail D, Joyce J. Microenvironmental regulation of tumor progression and metastasis. Nat Med. 2013;19(11):1423–37.

11. Torre LA, Bray F, Siegel RL, Ferlay J, Lortet-tieulent J, Jemal A. Global Cancer Statistics, 2012. CA Cancer J Clin. 2015;65:87–108.

12. J. Ferlay, I. Soerjomataram, R. Dikshit, S. Eser, C. Mathers, M. Rebelo, D.M. Parkin, D. Forman FB. Cancer incidence and mortality worldwide: sources, methods and major patterns in GLOBOCAN 2012. Int J Cancer. 2014.

13. Ferlay J, Soerjomataram I, Ervik M et al. GLOBOCAN 2012 v1.0, Cancer Incidence and Mortality Worldwide: IARC CancerBase No. 11 . Int Agency Res Cancer [Internet]. 2013; Available from: http://globocan.iarc.fr

14. Lemjabbar-Alaoui H, Hassan OU, Yang Y-W, Buchanan P. Lung cancer: Biology and treatment options. Biochim Biophys Acta; 2015;1856:189–210.

15. Yu H, Han Z, Wang Y, Xin H. The Clonal Evolution and Therapeutic Approaches of Lung Cancer. Cell Biochem Biophys. 2014;70:63–71.

16. Travis WD, Brambilla E, Nicholson AG, Yatabe Y, Austin JHM, Beasley MB, et al. The 2015 World Health Organization Classification of Lung Tumors: Impact of Genetic, Clinical and Radiologic Advances Since the 2004 Classification. J Thorac Oncol. International Association for the Study of Lung Cancer; 2015;10(9):1243–60.

17. Pirker R, Filipits M. Personalized treatment of advanced non-small-cell lung cancer in routine clinical practice. Cancer Metastasis Rev. 2016;35(1):141–50.

18. Sobin L, Gospodarowicz M WC (eds). TNM : classification of malignant tumours. Seventh Ed. Blackwell Publishing, Ltd; 2009. 1- 310.

19. Travis WD, Brambilla E, Riely GJ. New pathologic classification of lung cancer: Relevance for clinical practice and clinical trials. J Clin Oncol. 2013;31(8):992–1001.

20. Collisson EA, Campbell JD, Brooks AN, Berger AH, Lee W, Chmielecki J, et al. Comprehensive molecular profiling of lung adenocarcinoma. Nature. 2014;511(7511):543–50.

21. The Clinical Lung Cancer Genome Project (CLCGP);, (NGM) NGM. A Genomics-Based Classification of Human Lung Tumors. Sci Transl Med. 2013;5(209):1–28.

22. Shtivelman E, Hensing T, Simon GR, Dennis PA, Otterson GA, Bueno R, et al. Molecular pathways and therapeutic targets in lung cancer. Oncotarget. 2014;5(6):1392–433.

23. Pao W, Hutchinson KE. Chipping away at the lung cancer genome. Nat Med. Nature Publishing Group; 2012;18(3):349–51.

24. National Collaborating Centre for Cancer (UK). The diagnosis and treatment of lung cancer (update). NICE Clin Guidel. 2011;24.

25. Yasufuku K, Fujisawa T. Staging and diagnosis of non-small cell lung cancer: Invasive modalities. Respirology. 2007;12(2):173–83.

26. Yasufuku K, Fujisawa T. Staging and diagnosis of non-small cell lung cancer: Invasive modalities. Respirology. 2007;12:173–83.

27. Network NCC. NCCN Guidelines® [Internet]. 2011. Available from: https://www.nccn.org

28. Bordi P, Del Re M, Danesi R, Tiseo M. Circulating DNA in diagnosis and monitoring EGFR gene mutations in advanced non-small cell lung cancer. Transl lung cancer Res. 2015;4(5):584–97.

29. NCCN. Lung Cancer - Non-Small Cell lung cancer. NCCN Guidel Patients. 2016;409–36.

30. Howington JA, Blum MG, Chang AC, Balekian AA, Murthy SC. Treatment of stage I and II non-small cell lung cancer: Diagnosis and management of lung cancer, 3rd ed: American college of chest physicians evidence-based clinical practice guidelines. Chest. The American College of Chest Physicians; 2013;143(5 SUPPL):e278S – e313S.

31. Varela G, Thomas PA. Surgical management of advanced non-small cell lung cancer. J Thorac Dis. 2014;6(S2):S217–23.

32. Popper HH. Progression and metastasis of lung cancer. Cancer Metastasis Rev. 2016;35:75–91.

33. Lynch TJ, Patel T, Dreisbach L, McCleod M, Heim WJ, Hermann RC, et al. Cetuximab and first-line taxane/carboplatin chemotherapy in advanced non-small-cell lung cancer: Results of the randomized multicenter phase III trial BMS099. J Clin Oncol. 2010;28(6):911–7.

34. Ciuleanu T, Stelmakh L, Cicenas S, Miliauskas S, Grigorescu AC, Hillenbach C, et al. Efficacy and safety of erlotinib versus chemotherapy in second-line treatment of patients with

advanced, non-small-cell lung cancer with poor prognosis (TITAN): A randomised multicentre, open-label, phase 3 study. Lancet Oncol. 2012;13:300–8.

35. Shaw AT, Kim D-W, Nakagawa K, Seto T, Crinó L, Ahn M-J, et al. Crizotinib versus Chemotherapy in Advanced *ALK* -Positive Lung Cancer. N Engl J Med. 2013;368(25):2385–94.

36. Tang J, Salama R, Gadgeel SM, Sarkar FH, Ahmad A. Erlotinib resistance in lung cancer: Current progress and future perspectives. Front Pharmacol. 2013.

37. Choi YL, Soda M, Yamashita Y, Ueno T, Takashima J, Nakajima T, et al. EML4-ALK Mutations in Lung Cancer That Confer Resistance to ALK Inhibitors. N Engl J Med. 2010;16–21.

38. Topalian SL, Weiner GJ, Pardoll DM. Cancer immunotherapy comes of age. J Clin Oncol. 2011;29(36):4828–36.

39. Giaccone G, Bazhenova LA, Nemunaitis J, Tan M, Juh??sz E, Ramlau R, et al. A phase III study of belagenpumatucel-L, an allogeneic tumour cell vaccine, as maintenance therapy for non-small cell lung cancer. Eur J Cancer. 2015;51(16):2321–9.

40. Valecha GK, Vennepureddy A, Ibrahim U, Safa F, Samra B, Atallah JP. Anti–PD-1/PD-L1 antibodies in non-small cell lung cancer: the era of immunotherapy. Expert Rev Anticancer Ther. Taylor & Francis; 2017;17(13):47–59.

41. Salgia R. Mutation testing for directing upfront targeted therapy and post-progression combination therapy strategies in lung adenocarcinoma. Expert Rev Mol Diagn. 2016.

42. Vendrell J, Mau-Them F, Béganton B, Godreuil S, Coopman P, Solassol J. Circulating Cell Free Tumor DNA Detection as a Routine Tool forLung Cancer Patient Management. Int J Mol Sci. 2017;18(264).

43. Perakis S, Speicher MR. Emerging concepts in liquid biopsies. BMC Med. BMC Medicine; 2017;15(75).

44. Verma M. Personalized Medicine and Cancer. J Pers Med. 2012;2:1–14.

45. Crowley E, Di Nicolantonio F, Loupakis F, Bardelli A. Liquid biopsy: monitoring cancer-genetics in the blood. Nat Rev Clin Oncol. Nature Publishing Group; 2013;10(8):472–84.

46. Bryan A. Chan BGMH. Targeted therapy for non-small cell lung cancer: current standards and the promise of the future. Transl lung cancer Res. 2015;4(1):36–54.

47. Charles G. Mullighan, Letha A. Phillips, Xiaoping Su, Jing Ma CBM, Sheila A. Shurtleff and JRD. Genomic analysis of the clonal origins of relapsed acute lymphoblastic leukemia. Science (80-). 2009;322(5906):1377–80.

48. Mitnick CD, Shin SS, Seung KJ, Rich ML, Atwood SS, Furin JJ, et al. Intratumor Heterogeneity and Branched Evolution Revealed by Multiregion Sequencing. N Engl J Med. 2008;563–74.

49. Navin N, Kendall J, Troge J, Andrews P, Rodgers L, McIndoo J, et al. Tumor Evolution Inferred by Single Cell Sequencing. Nature. 2011;472(7341):90–4.

50. Alix-Panabieѐres C, Pantel K. Circulating tumor cells: Liquid biopsy of cancer. Clin Chem. 2013;59(1):110–8.

51. Luis A. Diaz Jr. Liquid Biopsies: Genotyping Circulating Tumor DNA. J Clin Oncol. 2014;32(6):579–86.

52. P. Mandel PM. Les acides nucleiques du plasma sanguine chez l'homme. C R Acad Sci Paris. 1948;241–3.

53. Leon SA, Shapiro B, Sklaroff DM, Leon SA, Shapiro B, Sklaroff DM, et al. Free DNA in the Serum of Cancer Patients and the Effect of Therapy. Cancer Res. 1977;37:646–50.

54. Cheng F, Su L, Qian C. Circulating tumor DNA: a promising biomarker in the liquid biopsy of cancer. Oncotarget. 2015;7(30).

55. Ai B, Liu H, Huang Y, Peng P. Circulating cell-free DNA as a prognostic and predictive biomarker in non-small cell lung cancer. Oncotarget. 2016;7(28):44583–95.

56. Lo YM, Zhang J, Leung TN, Lau TK, Chang AM, Hjelm NM. Rapid clearance of fetal DNA from maternal plasma. Am J Hum Genet. 1999;64:218–24.

57. Jiang P, Chan CWM, Chan KCA, Cheng SH, Wong J, Wong VW-S, et al. Lengthening and shortening of plasma DNA in hepatocellular carcinoma patients. PNAS. 2015;112(11):E1317–25.

58. Kornberg RD, Lorch Y. Twenty-five years of the nucleosome, fundamental particle of the eukaryote chromosome. Cell. 1999;98:285–94.

59. Mouliere F, Robert B, Peyrotte E, Del Rio M, Ychou M, Molina F, et al. High fragmentation characterizes tumour-derived circulating DNA. PLoS One. 2011;6(9).

60. Matthew W. Snyder, Martin Kircher, Andrew J. Hill RMD and JS. Cell-free DNA comprises an in vivo nucleosome footprint that informs its tissue-of-origin. Cell. 2016;164:57–68.

61. Jahr S, Hentze H, Englisch S, Hardt D, Fackelmayer FO, Hesch R. DNA Fragments in the Blood Plasma of Cancer Patients : Quantitations and Evidence for Their Origin from Apoptotic and Necrotic Cells. Cancer Res; 2001;1659–65.

62. Alix-Panabières C, Pantel K. Clinical applications of circulating tumor cells and circulating tumor DNA as liquid biopsy. Cancer Discov. 2016;6(5):479–91.

63. Schwarzenbach H, Hoon DSB, Pantel K. Cell-free nucleic acids as biomarkers in cancer patients. Nat Rev Cancer. Nature Publishing Group; 2011;11(6):426–37.

64. Thierry AR. A Targeted Q-PCR-Based method for point mutations testing by analizing cisculating DNA for cancer managment care. In: Clinical applications of PCR. 2016.

65. Diehl F, Schmidt K, Choti M a, Romans K, Li M, Thornton K, et al. Circulating mutant DNA to assess tumor dynamics. Nat Med. 2008;14(9):985–90.

66. Underhill HR, Kitzman JO, Hellwig S, Welker NC, Daza R, Baker DN, et al. Fragment Length of Circulating Tumor DNA. PLoS Genet. 2016;12(7):1–24.

67. Gahan PB. Circulating Nucleic Acids in Early Diagnosis , Prognosis and Treatment Monitoring, Advances in Predictive, Preventive and Personalised Medicine. ©Springer Science+Business Media Dordrecht, editor. 2015.

68. Madhavan D, Wallwiener M, Bents K, Zucknick M, Nees J, Schott S, et al. Plasma DNA integrity as a biomarker for primary and metastatic breast cancer and potential marker for early diagnosis. Breast Cancer Res Treat. 2014;146(1):163–74.

69. Frattini M, Gallino G, Signoroni S, Balestra D, Lusa L, Battaglia L, et al. Quantitative and qualitative characterization of plasma DNA identifies primary and recurrent colorectal cancer. Cancer Lett. 2008;263(2):170–81.

70. Sozzi G, Conte D, Mariani L, Vullo S Lo, Roz L, Lombardo C, et al. Analysis of Circulating Tumor DNA in Plasma at Diagnosis and during Follow-Up of Lung Cancer Patients Advances in Brief of Lung Cancer Patients. Cancer Res. 2001;61:4675–8.

71. Heitzer E, Ulz P, Geigl JB. Circulating tumor DNA as a liquid biopsy for cancer. Clin Chem. 2015;61(1):112–23.

72. Heitzer E, Auer M, Hoffmann EM, Pichler M, Gasch C, Ulz P, et al. Establishment of tumor-specific copy number alterations from plasma DNA of patients with cancer. Int J Cancer. 2013;133:346–56.

73. Leary RJ, Sausen M, Kinde I, Papadopoulos N, John D, Craig D, et al. Detection of Chromosomal Alterations in the Circulation of Cancer Patients with Wole-Genome Sequencing. Sci Transl Med. 2012;4(162):1–21.

74. Imamura F, Uchida J, Kukita Y, Kumagai T, Nishino K, Inoue T, et al. Monitoring of treatment responses and clonal evolution of tumor cells by circulating tumor DNA of heterogeneous mutant EGFR genes in lung cancer. Lung Cancer. 2016;94:68–73. Available from: http://dx.doi.org/10.1016/j.lungcan.2016.01.023

75. Newman AM, Bratman S V, To J, Wynne JF, Neville C, Eclov W, et al. An ultrasensitive method for quantitating circulating tumor DNA with broad patient coverage. Nat Med. 2014;20(5):548–54.

76. Dawson S-J, Tsui DWY, Murtaza M, Biggs H, Rueda OM, Chin S-F, et al. Analysis of Circulating Tumor DNA to Monitor Metastatic Breast Cancer. N Engl J Med. 2013;368(13):1199–209.

77. Spindler K-LG, Pallisgaard N, Vogelius I, Jakobsen A. Quantitative Cell-Free DNA, KRAS, and BRAF Mutations in Plasma from Patients with Metastatic Colorectal Cancer during Treatment with Cetuximab and Irinotecan. Clin Cancer Res. 2012;18(4):1177–85.

78. Riediger AL, Dietz S, Schirmer U, Meister M, Heinzmann-Groth I, Schneider M, et al. Mutation analysis of circulating plasma DNA to determine response to EGFR tyrosine kinase inhibitor therapy of lung adenocarcinoma patients. Sci Rep. Nature Publishing Group; 2016;6(33505).

79. Misale S, Yaeger R, Hobor S, Scala E, Liska D, Valtorta E, et al. Emergence of KRAS mutations and acquired resistance to anti EGFR therapy in colorectal cancer. Nature. 2012;486(7404):532–6.

80. Esposito A, Criscitiello C, En, Locatelli M, Milano M, Curigliano G. Liquid biopsies for solid tumors: Understanding tumor heterogeneity and real time monitoring of early resistance to targeted therapies. Pharmacol Ther. 2015;157:120–4.

81. Bidard FC, Madic J, Mariani P, Piperno-Neumann S, Rampanou A, Servois V, et al. Detection rate and prognostic value of circulating tumor cells and circulating tumor DNA in metastatic uveal melanoma. Int J Cancer. 2014;134(5):1207–13.

82. Shaw J, Page K, Blighe K, Hava N. Genomic analysis of circulating cell-free DNA infers breast cancer dormancy. Genome Res. 2012;(22):220–31.

83. Malapelle U, Pisapia P, Rocco D, Smeraglio R, di Spirito M, Bellevicine C, et al. Next generation sequencing techniques in liquid biopsy: focus on non-small cell lung cancer patients. Transl Lung Cancer Res. 2016;5(5):505–10.

84. Fleischhacker M, Schmidt B, Weickmann S, Fersching DMI, Leszinski GS, Siegele B, et al. Methods for isolation of cell-free plasma DNA strongly affect DNA yield. Clin Chim Acta; 2011;412(23-24):2085–8.

85. Devonshire AS, Whale AS, Gutteridge A, Jones G, Cowen S, Foy CA, et al. Towards standardisation of cell-free DNA measurement in plasma: Controls for extraction efficiency, fragment size bias and quantification. Anal Bioanal Chem. 2014;406(26):6499–512.

86. Page K, Guttery DS, Zahra N, Primrose L, Elshaw SR, Pringle JH, et al. Influence of Plasma Processing on Recovery and Analysis of Circulating Nucleic Acids. PLoS One. 2013;8(10):2–11.

87. Sonnenberg A, Marciniak JY, Rassenti L, Ghia EM, Skowronski EA, Manouchehri S, et al. Rapid electrokinetic isolation of cancer-related circulating cell-free DNA directly from blood. Clin Chem. 2014;60(3):500–9.

88. Taly V, Pekin D, Benhaim L, Kotsopoulos SK, Corre D Le, Li X, et al. Multiplex picodroplet digital PCR to detect KRAS mutations in circulating DNA from the plasma of colorectal cancer patients. Clin Chem. 2013;59(12):1722–31.

89. Kinde I, Wu J, Papadopoulos N, Kinzler KW, Vogelstein B. Detection and quantification of rare mutations with massively parallel sequencing. PNAS. 2011;108(23):9530–5.

90. Matikas A, Syrigos KN, Agelaki S. Circulating Biomarkers in Non-Small Cell Lung Cancer: Current Status and Future Challenges. Clin Lung Cancer. 2016;1–10.

91. David M. DiBardino DWR et al. Next-generation sequencing of non-small cell lung cancer using a customized, targeted sequencing panel: Emphasis on small biopsy and cytology. Cytojournal. 2017.

92. Gallego CJ, Shirts BH, Bennette CS, Guzauskas G, Amendola LM, Horike-Pyne M, et al. Next-generation sequencing panels for the diagnosis of colorectal cancer and polyposis syndromes: A cost-effectiveness analysis. J Clin Oncol. 2015;33(18):2084–91.

93. Malapelle U, Mayo de-Las-Casas C, Rocco D, Garzon M, Pisapia P, Jordana-Ariza N, et al. Development of a gene panel for next-generation sequencing of clinically relevant mutations in cell-free DNA from cancer patients. Br J Cancer. 2017;116(6):802–10.

94. Heitzer E, Ulz P, Belic J, Gutschi S, Quehenberger F, Fischereder K, et al. Tumor-associated copy number changes in the circulation of patients with prostate cancer identified through whole-genome sequencing. Genome Med. 2013;5(30).

95. Krishnamurthy N, Emily Spencer et al. Liquid Biopsies for Cancer: Coming to a Patient near You. J Clin Med. 2017;6(1).

96. E. A, A. S, A. M. DNA sequencing and bar-coding using solid-state nanopores. Electrophoresis. 2012;33(23):3437–47.

97. AstraZeneca. IRESSA receives CHMP positive opinion to include blood based diagnostic testing in European label. 2014. Available from: https://www.astrazeneca.com/media-centre/press-releases/2014/iressa-chmp-positive-opinion-blood-based-diagnostic-

testing-european-label-26092014.html#

98. Mok TS, Wu Y-L, Ahn M-J, Garassino MC, Kim HR, Ramalingam SS, et al. Osimertinib or Platinum–Pemetrexed in *EGFR* T790M–Positive Lung Cancer. N Engl J Med. 2017;376(7):629–40.

99. Suda K, Onozato R, Yatabe Y, Mitsudomi T. EGFR T790M mutation: a double role in lung cancer cell survival? J Thorac Oncol. International Association for the Study of Lung Cancer; 2009;4(1):1–4.

100. Hamed SS, Straubinger RM, Jusko WJ. Pharmacodynamic modeling of cell cycle and apoptotic effects of gemcitabine on pancreatic adenocarcinoma cells. 2014;72(3):553–63.

101. Richard A. Stanton, Kim M. Gernert, James H Nettles and RA. Drugs that target dynamic microtubules: a new molecular perspective. Med Res Rev. 2011;31(3):443–81.

102. Torres K, Horwitz SB. Mechanisms of taxol-induced cell death are concentration dependent. Cancer Res. 1998;58(16):3620–6.

103. Mhaidat NM, Wang Y, Kiejda K a, Zhang XD, Hersey P. Docetaxel-induced apoptosis in melanoma cells is dependent on activation of caspase-2. Mol Cancer Ther. 2007;6(2):752–61.

104. Tamatani T, Ferdous T, Takamaru N, Hara K, Kinouchi M, Kuribayashi N, et al. Antitumor efficacy of sequential treatment with docetaxel and 5-fluorouracil against human oral cancer cells. Int J Oncol. 2012;41(3):1148–56.

105. Nair AB, Jacob S. A simple practice guide for dose conversion between animals and human. J basic Clin Pharm. 2016;7(2):27–31.

106. Thierry AR, Mouliere F, Gongora C, Ollier J, Robert B, Ychou M, et al. Origin and quantification of circulating DNA in mice with human colorectal cancer xenografts. Nucleic Acids Res. 2010;38(18):6159–75.

107. Kyle AH, Huxham LA, Yeoman DM, Minchinton AI. Limited Tissue Penetration of T axanes : A Mechanism for Resistance in Solid T umors. Cancer Ther Preclin. 2007;13(9):2804–11.

108. Aubertin K, Silva AKA, Luciani N, Espinosa A, Djemat A, Charue D, et al. Massive release of extracellular vesicles from cancer cells after photodynamic treatment or chemotherapy. Sci Rep. Nature Publishing Group; 2016;6(October):35376.

APPENDIX 1

Table A1. Description of the material collected from each animal included in the study. Blood collected and respective fraction of plasma is presented. Tumor volume was measured at time of treatment.

			Blood		Tumor	
	Experimental groups	Animal ID	Total volume (µL)	Plasma volume (µL)	Tumor volume (mm^3)	Observations
	NX Control	21TD	?	600	-	
		190FED	800	465	-	
		191TED	700	380	-	
24h	NX DOC 10mg/Kg	188FE	600	510	-	
		187TD	900	480	-	
		174TDE	850	490	-	
	NX DOC 25mg/Kg	54FD	900	600	-	
		56FE	200	180	-	
		209FD	950	572	-	
48h	NX DOC 10mg/Kg	58FD	450	280	-	
		189TE	900	500	-	
		211FE	900	572	-	
	NX DOC 25mg/Kg	60FE	800	505	-	
		61TE	200	160	-	
		210TD	700	290	-	
	X Control	88	700	385	1195,21	
		100	800	460	1139,87	
		101	1000	510	1587,32	
		107	800	530	981,19	
		90	700	450	1142,56	
		108	750	445	1216,02	
24h	X DOC 10mg/Kg	92	800	510	1336,76	Ulceration
		105	800	540	1555,29	
		110	950	670	1205,62	Ulceration
		111	900	560	1300,44	Ulceration
		125	700	464	1265,22	
		137	800	530	1213,46	Ulceration
		199	700	450	1374,07	
	X DOC 25mg/Kg	91	600	400	1433,23	
		96	750	460	1535,36	
		98	750	480	1307,51	
		99	800	490	1086,07	Ulceration
		102	900	540	1383,76	
		140	1000	695	1100,02	Ulceration
48h	X DOC 10mg/Kg	131	650	430	1061,11	Ulceration
		129	450	310	1236,77	
		139	550	390	1310,16	
		127	900	585	1394,28	
		138	1000	555	1363,82	
		134	900	530	1221,38	Ulceration
	X DOC 25mg/Kg	126	400	290	1307,05	
		135	900	570	1496,64	
		142	900	575	1430,36	
		147	250	199	1357,41	
		141	1000	690	1462,36	Ulceration
		144	850	527	1203,54	
		214	700	410	1216,96	

NX: non-xenografted mice; X: xenografted mice; DOC: docetaxel.

APPENDIX 2

Digital PCR is a new approach which allow the amplification of single DNA fragments for quantification and rare allele detection. Results analysis give information on the number mutated and WT fragments for the target sequences.

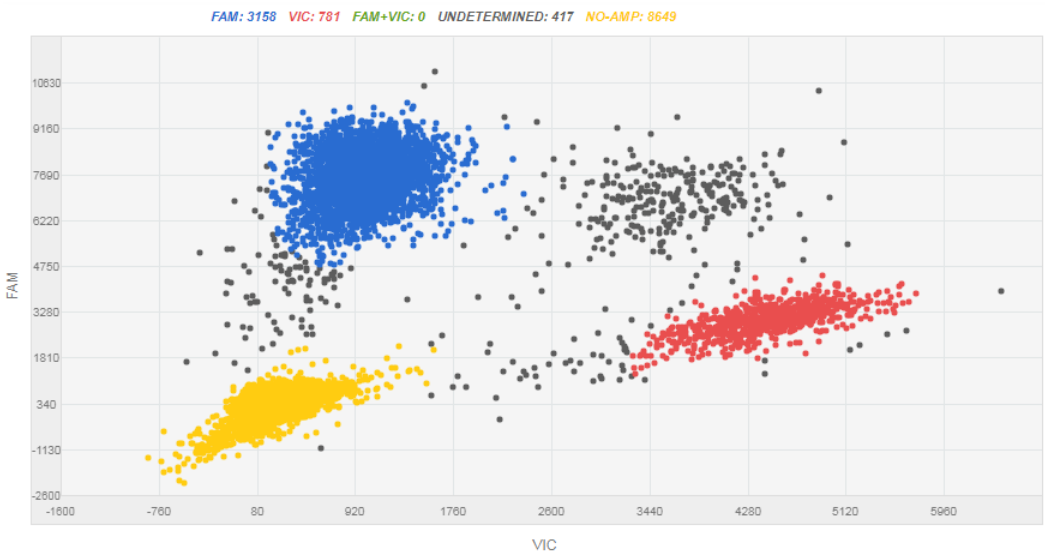

Figure A1. Representative image of the results obtained from digital PCR. DNA from H1975 cells-derived tumor. FAM: intensity of probe signal specific for mutated allele; VIC: FAM: intensity of probe signal specific for WT allele; Blue dots: mutated allele; Red: WT allele; Yellow: Empty wells; Grey dots: Undetermined signal.

APPENDIX 3

Table A2. Total and mutated DNA quantifications by quantitative PCR. Mean values of total ctDNA (T790M WT positive); mutated ctDNA (T790M positive) and mutational load values for each sample tested in the untreated and treated conditions.

		Total ctDNA	Mutated ctDNA	Mutational load
		(ng/mL of plasma)		(%)
	X Control	0.00	0.00	0.00
		0.52	0.00	0.00
24h	DOC 10mg/Kg	0.88	0.07	8.45
		1.35	0.23	16.63
		4.90	3.68	75.12
	DOC 25mg/Kg	2.00	0.53	26.75
		0.47	0.21	45.40
		7.20	3.05	42.35
48h	DOC 10mg/Kg	1.03	0.48	46.76
		5.38	2.40	44.70
		8.20	2.67	32.56
	DOC 25mg/Kg	2.20	0.18	8.27
		1.10	0.60	54.59
		0.87	0.25	28.42

X: xenografted mice; DOC: docetaxel.